THE UNITED NATIONS UNIVERSITY

ORKUSTOFNUN
NATIONAL ENERGY AUTHORITY

MULTIPLE FLUID - MINERAL EQUILIBRIUM CALCULATIONS AND THEIR APPLICATIONS TO GEOTHERMOMETRY AND HYDROCHEMICAL PROCESSES IN GEOTHERMAL SYSTEMS

Pang Zong-he

Geothermal Training Programme
Reykjavík, Iceland
Report 5, 1988

Report 5, 1988

MULTIPLE FLUID - MINERAL EQUILIBRIUM CALCULATIONS AND THEIR APPLICATIONS TO GEOTHERMOMETRY AND HYDROCHEMICAL PROCESSES IN GEOTHERMAL SYSTEMS

Pang Zhong-he
UNU Geothermal Training Programme
National Energy Authority
Grensasvegur 9
108 Reykjavik
ICELAND

Permanent Address:
Institute of Geology
Academia Sinica
P.O. Box 634, Beijing
PEOPLE'S REPUBLIC OF CHINA

ABSTRACT

Thermodynamic geochemical approaches based on theoretical calculations and modeling have become increasingly accurate as regards understanding the various processes occurring in hydrothermal systems. The log(Q/K) diagrams give an indication of the equilibrium state by comparing measured constituent concentrations with theoretical saturation activities over a range of temperatures. Using the results of chemical analyses the WATCH program has been employed to carry out calculations, the results of which have made it possible to construct log(Q/K) diagrams for geothermal and related natural waters from Iceland and China. In this way, it has been shown which minerals are possibly in equilibrium with the fluid constituents at certain temperatures. This approach facilitates the choice of geothermometers and provides a better understanding of the system; i.e. the processes that are responsible for the presence or absence of an equilibrium situation, e.g. the influence of seawater in the case of a coastal aquifer and other processes like boiling and mixing with shallow diluted water.

CONTENTS

TABLES

FIGURES

1. INTRODUCTION

Geothermal systems are complicated because of many thermal and chemical processes experienced by the thermal fluids rising to the surface from a deep reservoir. The present report begins with a short summary of the major processes which affect low temperature systems and a brief survey of the geochemical approaches used for understanding these processes.

Chemical equilibrium calculations have been made possible by the increasing thermodynamic data for many minerals found in geothermal systems. In recent geochemical work such calculations have been applied to geothermal investigations and such applications are the aim of the present project.

Sampling and analysis of geothermal fluids are very important parts of geochemical studies and their quality controls the accuracy of all consequent calculations. Geothermal fluid sampling from both low and high temperature wells, springs, fumaroles and laboratory analyses constitute the first part of the author's project work. A brief description of the work and some analytical methods used is included in this report.

The discussion of the geochemical methods brings us to the main point of the present report - the log(Q/K) diagram, a new approach to geothermometry and some hydrothermal processes that was first proposed by Reed and Spycher (1984). The theoretical background and the calculation procedures presented for the log(Q/K) approach and existing models are reviewed.

The computer programme WATCH that was used in the calculations for this report is described. Procedures for carrying out the calculations are explained and some factors that may influence the result of calculations are discussed with special emphasis on the effect of errors in pH

measurements.

The methodology for applying the log (Q/K) diagram to geothermometry and hydrothermal-chemical processes as suggested by the present author is discussed, followed by some case studies, either because they are of practical interest or as examples of low temperature geothermal areas of Iceland and China, which represent basaltic and granitic environments respectively.

Good understanding of the actual processes that take place in geothermal systems is shown to be very important by coupling different aspects of geothermal studies with geochemistry particularly as regards their site-specific features.

2. HYDROTHERMAL GEOCHEMICAL PROCESSES

2.1 General

Low temperature geothermal systems are widely distributed around the world and they are of interest especially for direct utilization. From a geological point of view, low temperature areas are located outside the active volcanic zones and are heated up by rocks with normal or fairly high heat flow.

A summary of water types found in geothermal systems is given by Henley (1984a). The chemistry of low temperature geothermal fluids is much simpler than that of high temperature ones. The origin of the thermal water is usually meteoric, but in some systems deep marine or some other saline waters (White, 1986) may be present. Geothermal systems near the coast may be fed by seawater or a mixture of seawater and meteoric water.

The chemistry of geothermal water in low temperature systems is mainly controlled by the reactions between thermal water and the host rocks and can be modified by hydrothermal processes such as boiling or mixing of thermal water with shallow groundwater.

2.2 Boiling

As hot water rises towards the surface the pressure on it by the overlying fluid decreases and a phase change - boiling of water may take place. The phase boundary is conventionally displayed as a boiling point - depth curve (Figure 2.1). Where boiling occurs there is a partitioning of dissolved constituents between the steam and the residual liquid; dissolved gases and other relatively volatile components concentrate in the steam and non-volatile components in the liquid in proportion to the amount of steam that separates.

2.3 Underground Mixing

Mixing of ascending hot with shallow cold groundwater in hydrothermal systems appears to be common. Mixing can also occur deep in hydrothermal systems, especially at the margins. (Fournier, 1977, 1979, 1981)

2.4 Hydrothermal Reactions

The composition of geothermal fluids is controlled by temperature-dependent reactions between minerals and fluids. Hydrolysis reactions are the most important but redox reactions occur too. If the residence time of the fluid is long enough, equilibria between the geothermal fluid constituents and the host rock may be reached. On the other hand, new equilibria may replace older ones if the system conditions change. In order to understand and model hydrothermal systems both the fluid constituents and the solids must be characterized.

3. GEOCHEMICAL APPROACHES

3.1 General

The most important geochemical approaches for understanding and modeling hydrothermal systems are:

* Comparison of conservative element concentrations (e.g. Cl) between wells and consideration of the effects of boiling and dilution (mixing diagrams).

* Relations between component ratios, concentrations and deep temperatures (Na/K, NaKCa, gas and silica geothermometers).

* Investigation of relations between the observed fluid chemistry and the alteration minerals found in the drillcores, based on thermodynamic data and highlighting the relationship between the different fluid components.

* Calculation of multi-component chemical equilibria and reaction processes in hydrothermal systems.

3.2 Geothermometers

Reviews of conventional geothermometers that have been used in geothermal exploration were given by Fournier (1981) and Truesdell (1984). The most important ones are listed in Table 3.1. Most of them are empirical with assumptions regarding particular mineral equilibria, which in some cases may not be dominant or even exist.

3.3 Models for Boiling and Mixing

If the rate of the upflow is fast enough for the cooling of the fluid to be considered as approximately adiabatic, the final concentration C_f, of the remaining components in the

residual liquid after one-stage steam separation at a given temperature, t_f, is given by the formula

$$C_f=(H_s-H_f)/(H_s-H_i)*C_i$$

where C_i is the initial concentration before boiling, H_i is the enthalpy of the initial liquid before boiling and H_f and H_s are the final enthalpies of the final liquid and steam respectively at t_f.

Mixing models have been used in cases where hot water mixes with cold water. Examples of such models using Si and Cl analytical results are shown in Figure 3.1.

3.4 Hydrolysis Reaction Studies

Thermodynamic calculations for hydrolysis reactions were summarized by Henley (1984b). Reactions between water and different minerals can be studied and thus can different fluid systems. Activity - activity diagrams can be drawn for different mineral assemblages from thermodynamic data. The diagram can then be used to see whether different minerals can co-exist as a mineral assemblage under certain conditions. Some of the thermodynamic data is listed in Table 3.2 and a typical activity-activity diagram is shown in Figure 3.2.

3.5 Chemical Equilibrium Calculations

Many geochemical systems can be understood in terms of the reaction of an aqueous phase with its mineral environment. These systems can be studied by calculating the properties of heterogeneous chemical equilibrium among minerals, gases and aqueous solutions for a specified bulk composition, temperature and pressure. By linking a series of calculations in which incremental changes of bulk composition, temperature or pressure are made, one can produce a chemical model of a dynamic geochemical process.

Thermodynamic data for whole system geochemical calculations of this kind have become available in recent years.

Reed (1982) has developed a new approach that can model geochemical processes involving composition changes by linking a series of discrete overall heterogeneous equilibrium calculations.

In many geochemical studies, it is necessary to use results of analyses and pH measurements made at room temperature and pressure. The measured chemical properties in such cases are different from those at high temperature and pressure because of gas separation, mineral precipitation, and temperature dependence of homogeneous equilibria. There are several methods available for calculating pH at high temperature from analytical results at low temperature, (Wilson, 1961; Arnorsson et al., 1982). All rely on estimates of "total ionizable hydrogen". A method presented by Reed and Spycher (1984) employing multi-component equilibrium calculations requires no judgment about "ionizable hydrogen" since it readily takes account of all H^+ species and the effect of dissolved gases.

The latest developments in the field of chemical equilibrium calculations have benefited geothermal studies, but there are still some crucial limitations, one of them arises from the fact that in low temperature geothermal studies one has to deal with many kinds of clay minerals. The thermodynamic data necessary for natural clay minerals (especially those that contain impurities) are insufficient at the moment and this may cause difficulty in calculations of this kind.

4. GEOTHERMAL SAMPLING AND CHEMICAL ANALYSES

4.1 Introduction

Sampling and analysis of geothermal fluids are very important parts of geochemical studies, and their results control the accuracy of all the successive calculations. Geothermal fluid sampling from both low and high temperature wells, springs and fumaroles was practiced during this training and so was the analysis of some important constituents of the samples collected, in the laboratory of the National Energy Authority of Iceland. A brief description of the work and some of the analytical methods used follows.

4.2 Low Temperature Samples

One hot spring water sample was collected from England, in the Borgarfjordur geothermal area at a temperature of around 90 °C. Three water samples from well number 2 of Seltjarnarnes field were taken from depths of 80, 570 and 725 meters respectively, using a downhole sampler. A cold spring in Thvera, Borgarfjodur was also sampled. The method of collection is shown in Figure 4.1.

The sample portions are as follows:

Ru, raw untreated, 250ml in gas sampling tubes made of glass for the determination of pH and CO_2.

Fu, filtered untreated, 200 - 500ml in plastic bottles for the determination of Cl and other anions.

Fd, filtered and diluted, 100ml in plastic bottles for silica determination, diluted 2 - 10x with distilled water to bring the silica concentration below 100ppm.

Fa, filtered and acidified, 100 - 500ml in plastic bottles for Na, Ca, Mg, Li, Al, Fe and Mn determinations.

The chemical analyses of the volatile constituents like pH, H_2S, CO_2 were done by the author soon after collection. The methods used are as follows:

pH was measured with a pH meter with a glass electrode.

Total carbonate as CO_2 was measured by titration with 0.1N HCl from pH 8.2 to 3.8, adjusting the initial pH with HCl and NaOH.

H_2S was determined by titration with 0.001 $Hg(CH_3COO)_2$ solution using dithizone as an indicator.

SiO_2, Fe,and Mn were determined spectrophotometrically.

Cl was determined by titration with $AgNO_3$.

Al was measured fluorimetrically.

4.3 High Temperature Samples

Sampling of two fumaroles in the Krafla area and one steam well, well number KG-24 was attended by the author. The method used is described by United Nations Development Programme (1986).

Three steam sample portions were collected from each fumarole and the steam well: The condensate of the fumarole steam, the non-condensable gas and the total fumarole steam dissolved in NaOH solution. Methods for collecting the samples were described by Armannsson (1985) and are shown in Figure 4.2.

A liquid water sample was also drawn from the well and divided into similar portions as the low temperature samples, with the addition of a portion labeled Fp (filtered, precipitated), where 10ml 0.2M $Zn(CH_3COO)_2$ are added to

490ml of sample to remove sulfide. This portion is used for sulphate analysis.

pH, H_2S and CO_2 were determined in the field laboratory of the Krafla geothermal power plant.

pH was measured with a pH meter.

H_2S was determined by titration with $Hg(CH_3COO)_2$ solution using dithizone as an indicator.

CO_2 was measured by titration with 0.1N HCl from pH 8.2 to 3.8 at room temperature.

5. THE LOG(Q/K) DIAGRAM

5.1 Theoretical Background and Established Models

Using the activities of aqueous component species calculated for homogeneous equilibrium at a series of temperatures, it is possible to compute the degree of super- or undersaturation of the aqueous phase with minerals at each temperature. This is expressed for mineral k in terms of $\log(Q/K)_k$:

$$\log(Q/K)_k = \log \prod a_{i,k}^{v_{i,k}} - \log K_k$$

in which Q is the calculated ion activity product and K is the equilibrium constant for mineral k, $a_{i,k}$ is the activity and $v_{i,k}$ is the stoichiometric coefficient of component species i in the equilibrium mass action expression for mineral k, written with the mineral on the left hand side.

Therefore, the log (Q/K) value for each mineral provides a measure of the proximity of the aqueous solution components to attaining equilibrium with the mineral. The numerical value of log(Q/K) is greater than zero for supersaturated minerals and less than zero for undersaturated minerals.

The increasing and improved thermodynamic data for various species in aqueous solutions and the established numerical methods mentioned above have made it possible to calculate the log(Q/K) value for many minerals using analytical values for the chemical components of geothermal fluids.

If an aqueous solution is in equilibrium with respect to a certain mineral assemblage, the temperature at which the components reach equilibrium can be identified. An ideal case (Figure 5.1) was given by Reed and Spycher (1984). The minerals that equilibrate with the fluid intersect the log(Q/K) = o line at the same temperature (250°C), but others do not.

This characteristic of convergence of log(Q/K) curves for the equilibrium assemblage to zero at the temperature of equilibration establishes a basis for geothermometry.

Effects of boiling and dilution of geothermal waters are discussed by Reed and Spycher (1984).

Boiling causes irregular dispersion of log(Q/K) curves because of the combined effects of concentration of aqueous components by water loss and pH change due to CO_2 loss. An example of this effect is shown in Figure 5.2.

In contrast, dilution causes a simple shift and dispersion of the mineral log(Q/K) curves which is readily recognized. The locus of most curve intersections (with log(Q/K) = 0) is displaced towards lower temperatures as is shown in Figure 5.3. The dilution considered here is the effect of mixing of a deep, hydrothermal solution with a relatively pure water.

5.2 The Computer Program WATCH

The computer program used in this study is the WATCH program of Arnorsson et al. (1982), which was developed to calculate the composition and aqueous speciation of geothermal reservoir waters including pH, redox potential and gas pressures. The program is specially suited to handle geochemical data from wet-steam wells, hot-water wells and boiling hot springs, but it may also be used for non-thermal waters.

Solubility data for 26 minerals commonly found in geothermal systems in Iceland were incorporated (Table 5.1 and Figure 5.4) to facilitate the study of fluid - mineral equilibria. Guides for the operation of the program were written by Svavarsson (1981) and Olafsson (1987).

The WATCH program comes in two parts, WATCH1 that can be used

with the results of chemical analyses of water and steam from steam producing wells, and WATCH3 that is exclusively used for the results of chemical analyses of water from boiling springs, hot springs and cold water. An example of a printout from WATCH3 is shown in Appendix I.

5.3 Preparation of the Log (Q/K) Diagram

The procedure for drawing the log (Q/K) diagrams is as follows:

* Use the log solubility products data from the WATCH program's printout to calculate the log (Q/K) values at selected temperatures. An example of such data is given in Appendix II.

* Use the calculated data to plot log (Q/K) against temperature for all minerals. An example of such a diagram is shown in Figure 5.5.

It is convenient to use the conventional geothermometer temperatures that are calculated by the WATCH program as a reference for the choice of temperature range for the calculation.

5.4 Interpretation of the Log(Q/K) Diagrams

5.4.1 Visual Specification

Visual interpretation of the diagrams gives us an impression of possible equilibria between the fluid constituents and the minerals or, if not, how close they are to equilibrium.

The number of mineral curves that cross the zero log (Q/K) horizontal line at the same temperature, or the number of minerals that co-exist in equilibrium is not great, 5 - 6 is the maximum in most cases.

5.4.2 Statistical Approach

Since different minerals may not reach equilibrium at exactly the same temperature, statistical methods can be used to search for the temperature range(s) where most minerals cross the horizontal zero line (Figure 5.6)

For cases where equilibrium curves for different minerals do not converge in the diagrams, statistical methods can be used to estimate the temperature range within which most of the minerals apparently equilibrate (Figure 5.7)

5.5 Basic Characteristics of the Log(Q/K) Diagram

5.5.1 Types of Curves

There are five types of curves classified by their slopes as they appear on the diagram shown in Figure 4.5 and listed in table 5.2. These curves of different slopes reflect their thermodynamic characteristics. Therefore, the indication of a possible equilibrium should be more reliable if the minerals that converge on the zero log(Q/K) line are of different types.

5.5.2 Effects of Mixing and Boiling

The effects of mixing and boiling discussed by Reed and Spycher (1984) were also evaluated by using the WATCH program with reference to a hot spring sample from Nanjin, China as an example. The results of such calculations as shown in Figures 5.8 and 5.9 are quite similar to those proposed by Reed and Spycher (1984). It seems possible that an optimum possible equilibrium can be attained by iteration calculations (with help the of a computer program).

5.6 Results for Some Natural Waters

Log (Q/K) calculations were performed with analytical data on

samples of different natural water types from the Zhangzhou geothermal area, Southeast China (Figure 5.10). The diagrams (Figures 5.11 - 5.13) show that the constituents of rainwater, riverwater, seawater and ambient temperature groundwater do not approach fluid-mineral equilibria.

5.6.1 Surface and Rain Waters

Images that imply the absence of equilibrium are seen in the results of the calculations for cold surface waters. Figures 5.11 and 5.12 show the diagrams for rainwater, seawater and riverwater from the same region.

5.6.2 Groundwater of Ambient Temperature

Cold groundwater is in most cases not in equilibrium with its host rock. This can be clearly seen in the diagrams in Figures 5.12 and 5.13. But convergent points far below the log(Q/K)=0 line reflect some possible ancient equilibria.

5.6.3 Geothermal Water

Calculations based on the results of chemical analyses of geothermal samples from Iceland and the Zhangzhou area, China were performed and the results show that the constituents of geothermal waters are in many cases quite close to equilibrium even though no exact equilibria can be identified. Figure 5.5 is an example of a calculated equilibrium situation. More detailed summary of the calculated results will be given in Chapter 6.

5.7 The Effect of Mixing with Seawater

The effect of the mixing of geothermal water with seawater can be seen quite clearly in a log(Q/K). This is a process that occurs widely in coastal geothermal areas in Iceland and China. This effect is evaluated for the geothermal water samples from the Zhangzhou geothermal area, Southeast China.

The log(Q/K) curves for minerals that are closely related to the seawater components are highly elevated above the log(Q/K) = 0 line (Figure 5.14).

5.8 Factors Affecting the Convergence of Mineral Curves

The effect of analytical errors on the calculations was tested in this study. In general, an ionic balance of less than 10% will give good results. But a simple approximation of analytical errors on all particular constituents or sets of them is not easily made.

The influence of an error in the measurement of pH on the results was calculated for a Chinese hot spring sample from Nanjin, Southeast China. Results show that the change of pH (measured at air temperature) by 0.1 unit would not make any difference, a slight difference is caused by 0.2 units, but a change of 0.5 pH units will cause significant differences, which can be seen in the diagrams (Figure 5.15).

Statistical methods were used to evaluate this effect (Figure 5.16). In diagrams where the same number of minerals reach equilibrium, a minimum value is obtained for the standard deviation, which can be regarded as a measure of the extent to which the curves for individual minerals cluster on the zero line. This minimum value may be called the "optimum statistical equilibrium". In Figure 5.16 it can also be seen that the equilibrium temperature does not change significantly within a pH change of 0.4 units.

Log(Q/K) diagrams only provide us with an impression of possible equilibria between the thermal fluid constituents and the minerals considered. An actual mineral assemblage has to be studied before any conclusion about real equilibria can be reached. This will be discussed in the following chapter.

6. METHODOLOGY FOR APPLICATIONS

6.1 Introduction

The computations discussed above provide us with an overall look at the studied system in terms of chemical equilibria between geothermal fluid constituents and minerals. The main purpose of the following discussion is to show how they benefit the use of geothermometers and the understanding of the hydrothermal system studied. Mineralogical and hydrogeological aspects will be discussed with examples from Iceland and China.

All the conventional geothermotmeters reviewed in Chapter 2 have the basic assumption in common, that the solution constituents studied are in equilibrium with the particular mineral or mineral assemblage considered and this can not be verified by the geothermometers themselves. The log (Q/K) diagram can be used to get an impression of possible equilibria between the aqueous solution components and the minerals. The present study shows that it has to be coupled with alteration mineral studies and/or hydrogeological information about the studied area before a conclusion about the subsurface temperature and the history of the thermal fluids can be drawn with confidence.

6.2 Coupling with Alteration Mineral Studies

The possible equilibria noted in the log(Q/K) diagrams should be tested to determine the plausible fluid - mineral equilibria. There are two ways of doing this.

* Mineral stability calculations using thermodynamic data to evaluate the possibility of the co-existence of particular mineral assemblages.

* Comparison of the minerals calculated to be in possible equilibrium with the alteration minerals

found in the geothermal wells.

The first method is useful for hot spring areas which have not been drilled. An example of the activity-activity diagrams was given in Chapter 3 and Figure 3.2. The second method can be used for gaining useful information from drillholes in different geothermal environments (conditions) which then can aid the choice of suitable geothermometers.

Examples from Iceland and China will be discussed in the following section. A general view of the alteration mineral studies of Icelandic low temperature ares will be given and and some fields discussed. An example from southeast China will also be presented.

The alteration minerals commonly found in active geothermal systems were summarized (Figures 6.1) by Henley & Ellis (1983). Those minerals used in the WATCH program are the ones that are most often found in Icelandic geothermal fields of different temperature. Summaries of these minerals and the common temperature ranges were given by Arnorsson et al. (1983) as shown in Figure 6.2, which gives one a general idea of the minerals or mineral assemblages that can reasonably be expected in the Icelandic systems. But different combinations of minerals are found in different areas.

6.3 Coupling with Hydrogeological Considerations

The effects of various hydrogeological processes on the use of conventional geothermometers were thoroughly discussed by Fournier (1979). The present concern is how the necessary considerations of hydrogeological information can benefit the log(Q/K) approach. Examples and preliminary discussion will follow.

In non-equilibrium cases, mixing and boiling may be the main factors that cause the non-convergence of the curves, as has been discussed in the previous sections of this report. On

the other hand, geothermal water in different parts of the flow (circulation) system shows different characteristics in terms of equilibria, since we know whether the equilibria shown in a log(Q/K) diagram reflect the most recent situation of the fluid.

Reykjanes geothermal area is a low temperature area located on a tiny peninsula in Isafjardardjup, West Iceland (Figure 6.3), with a natural outflow of more than 10 liters per second of hot water. The highest subsurface temperature measured is 98°C (Bjornsson et al., 1987).

Analytical results for samples from different parts of the flow system (Benjaminsson, 1981) were used to calculate the log(Q/K) diagrams. Thr results of the calculations show that the closer to the discharge area the sampling point is, the closer it is to equilibrium (see Figure 6.4 and also Table 7.1).

Therefore, if samples from different parts of the system are available, it is helpful to the understanding of the system to do the same calculations for all the samples and interpret them together.

7. CASE STUDIES FROM ICELAND AND CHINA

7.1 General

The analytical results for about 50 water samples from Iceland and China were used in this study. The Icelandic data are from the published paper of Arnorsson et al (1983) and the National Energy Authority of Iceland. The locations of the Icelandic samples are shown in Figure 7.1. These data represent the low temperature geothermal water in basalt of Quaternary and Tertiary origin.

Data of the Chinese geothermal water and related natural waters used here was taken from a technical report of a co-operative study between French and Chinese geothermal scientists (Demange et al., 1986), represent a coastal geothermal area in a granitic environment. The samples were collected from geothermal wells in the Zhangzhou geothermal field and some hot springs around the area, which is shown in Figure 5.10.

A summary of the results of the log(Q/K) calculations is shown in Tables 7.1 and 7.2. Results were coupled with information from other methods for the cases of equilibrium. Non-equilibrium can explained by effects of boiling, dilution and the contamination by seawater.

7.2 Leira Area, West Iceland

The geothermal area is located in the Tertiary basaltic environment. Alteration products in wells suggest a high temperature geothermal system bearing little relation to the present situation (Tomasson and Kristmannsdottir, 1974). Four wells have been drilled in this region and a sample from well 4 was used for mineral equilibrium calculations. The fluid is a relatively saline, calcium-rich, carbon dioxide water, δD = -73.8 and could be derived from water that has fallen as rain to the west of the Langjokull glacier, which is thought to be

the origin of the water in the other Borgarfjordur geothermal area. Arnason (1976) concludes that this is the case and that the salinity is derived from the leaching of salty sediments. On the other hand this water could originate from a heavier water that mixed with seawater a long time ago and ion exchange with rocks has produced the present composition (Armannsson, 1981).

Well number 4 is 2019 meters deep, the flow rate was 8 liters per second, discharge temperature was 128 °C. The log(Q/K) diagram for this well is shown in Figure 7.2, which indicates clearly a possible equilibrium of five or six minerals at a temperature of 165 °C. The minerals are two montmorillonites, chalcedony, analcime and wairakite - a kind of zeolite. A comparison of this with the alteration minerals (Figure 7.3) shows that the calculated fluid - mineral equilibria are likely to a realistic. The well has more than one inflow zones as shown in Figure 7.4. The calculated temperature seems to be in agreement with the chalcedony temperature (161.9°C), but not with the NaK and quartz geothermometers.

7.3 Zhangzhou Geothermal Area, Southeast China

7.3.1 Nanjin Hot Spring

The Nanjin hot spring area is located about 30 kilometers to the west of the Zhangzhou geothermal field. The total natural flow rate of hot water from hot springs in this area is greater than 20 liters per second.

The log(Q/K) diagram for a sample from a spring with the highest temperature of the area (Figure 7.5) shows the convergence of five possible mineral equilibria to the same temperature. The minerals are two montmorillonites, chalcedony, fluorite and calcite, representing quite a reasonable mineral assemblage to equilibrate with the host rock at a low temperature.

A 628 meters deep drillhole has been drilled in the vicinity of the spring and the measured downhole temperature was around 90 °C, which is in very good agreement with the temperature calculated here.

7.3.2 Zhangzhou Geothermal Field

In the case of a coastal aquifer, the geothermal fluid is a relatively concentrated seawater mixture, which raises the concentration of Cl, Na, and other elements. The construction of log(Q/K) diagrams for hot water samples from the Zhangzhou area, a costal hydro-thermal basin in southeastern China and its surroundings provides a better understanding of the mixing process and facilitates the choice of suitable geothermometers.

Geochemical and isotopic studies revealed that the saline hot water in this region is a mixture of meteoric water (Figure 7.6) and seawater (Demange et al., 1986; Pang, 1987). A series of samples of different salinity were used to calculate the mineral equilibria and plot the log(Q/K) diagrams. Results show that the curves for Na, K, Mg related species are highly elevated in the diagrams, which means that the these components in the water are dominated by seawater. The more saline the water, the more elevated the curves (see Figure 5.14).

It was doubted that the water components had reached equilibrium with respect to certain minerals, for the NaK geothermometers give very scattered results for reservoir temperature and that indicates a deviation from the actual situation where the presence of the particular minerals is inherent in the use of the geothermometers.

The data from this area was also plotted in the Giggenbach diagram (Giggenbach, 1986) which was designed to recognize a mineral assemblage of K-feldspar, illite and chlorite. The result shows that the seawater-dominated geothermal fluids do

not fall on the equilibrium curve in the diagram (Figure 7.7).

However, as is summarized in Table 7.2, the chalcedony geothermometer temperature is quite close to the reservoir temperature. In most of the log(Q/K) diagrams for this area, it can be seen that calcite and chalcedony cross the log(Q/K) = 0 line at the same or similar temperature. This indicates that these minerals are the ones that equilibrate with the host rock in this case and they are also the alteration minerals found widely in the geothermal area. Therefore, it is suggested that silica geothermometers be used in a coastal geothermal area like this one.

8. CONCLUSIONS

By using the chemical equilibrium computer program WATCH and plotting the log(Q/K) diagrams, possible equilibrium and non-equilibrium situations between studied fluid components and minerals can be identified for natural waters.

Chemical analysis with an ionic balance difference of less than 10% gives good results in most cases. An error of less than 0.2 units in pH measurement at the laboratory temperature does not cause a significant difference in the log(Q/K) diagrams.

Coupling the log(Q/K) diagrams with the results of alteration mineral studies and/or activity - activity diagrams shows for which minerals equilibrium is to be expected, and thus which geothermometers are applicable, making the geothermometry results more reliable than those obtained indiscriminately by conventional methods.

Hydrothermal-chemical processes can be modeled to certain extent by using the log(Q/K) diagrams.

Results for chemical analyses of water samples from Iceland and China show that this approach can benefit the study of different types of natural water(s) from the same region and aid the understanding of whole system.

ACKNOWLEDGEMENTS

The author wishes to thank his advisor, Dr. Halldor Armannsson of the National Energy Authority of Iceland for his guidance in this project work. Thanks are also due to Professor Stefan Arnorsson of the University of Iceland and Dr. Robert O. Fournier, the UNU guest lecturer for their helpful discussions with the author.

Special thanks are due to Dr. Jon-Steinar Gudmundsson, the director of the Geothermal Training Program for his successful operation of the program and the help the author has enjoyed from him during the training and this project work.

Mr. Magnus Olafsson is thanked for his help with the use of the WATCH program.

The author is indebted to many people of the National Energy Authority of Iceland, especially the people from the training programme and those of the geochemical laboratory that have provided help to the author in various ways.

This training of the author was supported by the United Nations University geothermal training programme and the Icelandic Government and was carried out in Reykjavik, Iceland.

NOMENCALTURE

a = Activity of aqueous species (moles/kg)
C = Concentration of chemical components (ppm)
H = Enthalpy (kJ/kg)
K = Theoretical equilibrium constant
M = Molal unit of chemical components (moles/kg of solvent)
N = Equivalents per liter
P = Pressure (bar)
pH = Negative log of hydrogen ion activity
Q = Calculated log solubility products
T = Temperature (°C)
v = Stoichiometric coefficient of species
wt% = Weight percent

$\delta D = H^2/H^1$ ratio with reference to SMOW (standard mean ocean water)

REFERENCES

Armannsson, H., 1981, Leira, Borgarfjordur, Chemical composition of borehole fluids and possibilities of deposition. Report OS81028/JHD16, National Energy Authority (in Icelandic), 53 pp.

Armannsson, H., 1985, A field guide to sampling of high temperature wells, selected analytical procedures and preliminary composition calculations, VIRKIR/NEA.

Arnason, B., 1976, Ground water systems in Iceland traced by deuterium. Icelandic Sci. Soc. Publication, 42, 236 pp.

Arnorsson, S., Sigurdsson, S. and Svavarsson, H., 1982, The chemistry of geothermal waters in Iceland. I. Calculations of aqueous speciation from 0° to 370°C, Geochim. Coschim. Acta 46, 1515-1532.

Arnorsson, S., Gunnlaugsson, E. and Svavarsson, H., 1983, The chemistry of geothermal waters in Iceland II. Mineral equilibria and independent variables controlling water compositions, Geochim. Coschim. Acta, 47, 547-566.

Benjaminsson, J., 1981, The Northwestern Peninsula, Iceland, Chemistry of geothermal waters, Report OS81010/JHD06, National Energy Authority (in Icelandic), 121 pp.

Bjornsson, G., Hersir, G. P. and Smarason, O. B., 1987, Well test of drillhole 2 of Reykjanes area, Report GrB/GPH/OBS-87/02, National Energy Authority (in Icelandic).

Demange, J.,Fabriol, R., Tournaye, D., 1986, Geothermal potential assessment of Zhangzhou area, Fujian province, People's republic of China, 86 CFG 022, 40 pp.

Fournier, R., 1977, Chemical geothermometers and mixing models for geothermal systems, Geothermics, 5, 31-40.

Fournier, R., 1979, Geochemical and hydrologic considerations and the use of enthalpy-chloride diagrams in the prediction of underground conditions in hot spring systems, J. Volc. Geotherm. Res., 5, 1-16.

Fournier, R. 1981, Application of water chemistry to Geothermal Exploration and Reservoir Engineering, Chapter 4 in: Geothermal Systems, Principles and case histories, Editors: Rybach, L., and Muffler, L. J. P., 109 - 140.

Giggenbach, W., 1986, Graphical techniques for the evaluation of the water/rock equilibration conditions by use of Na, K, Mg and Ca contents of discharge waters, Proc. 8th NZ geothermal workshop, 37 - 43.

Haas, J. L., 1971, The effect of salinity on the maximum thermal gradient of a hydrothermal system at hydrostatic pressure: Econ. Geol. 66, 940 - 946.

Helgesson, H. C., Delany, J. M., Nesbitt, H. W. and Bird, D. K., 1978, Summary and critique of the thermodynamic properties of rock forming minerals: Am. J. Sci. 274, 1199 - 1261.

Henley, R., 1984a, Chemical structure of geothermal systems, Chapter 2 in: Henley, R. W., Truesdell, A. H. and Barton, P. B., Fluid - mineral equilibria in hydrothermal systems, Reviews in Economic Geology, Vol. 1 (Robertson, J., series editor), Soc. Econ. Geol., 9 - 28.

Henley, R. W., 1984b, Hydrolysis reactions in hydrothermal fluids, Chapter 6 in: Henley, R. W., Truesdell, A. H. and Barton, P. B., Fluid-mineral equilibria in hydrothermal systems, Reviews in Economic Geology, Vol. 1 (Robertson, J., series editor), Soc. Econ. Geol., 65 - 82.

Henley, R. W. and Ellis, A. J., 1983, Geothermal systems,

ancient and modern: a geochemical review: Earth Sci. Reviews, 19, 1 - 50.

Olafsson, M., 1987, How to operate the WATCH and the PRI programmes -- an instructional manual, National Energy Authority of Iceland.

Pang, Z., 1987, Zhangzhou basin geothermal system - genesis model, energy potential and the occurrence of thermal water, Ph.D. disertation, Inst. Geol., Academia Sinica (in Chinese with English abstract), 310 pp.

Reed, M., 1982, Calculation of multi-component chemical equilibria and reaction processes in systems involving minerals, gases and aqueous phase, Geochim. Cosmochim. Acta, 46, 513-528.

Reed, M. and Spycher, 1984, Calculation of pH and mineral equilibria in hydrothermal waters with application to geothermometry and studies of boiling and dilution, Geochim. Cosmochim. Acta, 48, 1479-1492.

Svavarsson, H., 1981, The "WATCH1" and "WATCH3" programmes. A Guide for Users. National Energy Authority of Iceland.

Tomasson, J. and Kristmannsdottir, H., 1974, Leira, Well No. 4, Report OSJHD7551, National Energy Authority (in Icelandic), 22 pp.

Truesdell, A., 1984, Chemical geothermometers for geothermal exploration, Chapter 3 in Henley, R. W., Truesdell, A.H. and Barton, P. B., Fluid - mineral equilibria in hydrothermal systems, Reviews in Economic Geology, Vol. 1 (Robertson, J. M., series editor), Soc. Econ. Geol., 31 - 43.

United Nations Development Programme, 1986, Geothermal sampling and chemical analyses, Project: Exploration for Geothermal Energy KEN/82/002 - UN/DTCD.

White, D. E., 1986, Subsurface waters of different origins, Fifth international symposium on water-rock interaction (extended abstracts), Intern. Assoc. Geoch. Cosmoch. and National Energy Authority of Iceland, 629 - 632.

Wilson, S., 1961, pH of a natural hydrothermal solution, Geochim. Coschim. Acta, 25, 233-235.

Appendix I. An example of a printout from the WATCH program (WATCH3).

```
8511158-14                    Nanjin, hot spring - 1

PROGRAM WATCH2.

WATER SAMPLE (PPM)            STEAM SAMPLE

PH/DEG.C        8.24/25.0     GAS (VOL.%)                REFERENCE TEMP.     DEGREES C    180.0 (ARBITRARY)
SIO2           73.31          CO2
NA            139.46          H2S                        SAMPLING PRESSURE   BARS ABS.
K               2.49          H2                         DISCHARGE ENTHALPY  MJOUL/KG
CA              4.29          O2                         DISCHARGE           KG/SEC.      17.4
MG               .100         CH4
CO2           119.58          N2                         MEASURED TEMPERATURE DEGREES C   78.5
SO4           133.52                                     RESISTIVITY/TEMP.   OHMM/DEG.C    .0/  .0
H2S              .00                                     EH/TEMP.            MV/DEG.C      .000/  .0
CL             25.70
F              15.00          LITERS GAS PER KG
DISS.SOLIDS   455.66          CONDENSATE/DEG.C              MEASURED DOWNHOLE TEMP.   FLUID INFLOW
AL               .1220                                       DEGREES C/METERS        DEPTH (METERS)
B                .1490
FE               .0260        CONDENSATE (PPM)              .0      .0      .0
NH3              .0000        PH/DEG.C                      .0      .0      .0
                              CO2                           .0      .0      .0
                              H2S                           .0      .0      .0
                              NA                            .0      .0      .0
                                                            .0      .0      .0
                                                            .0      .0      .0
                                                            .0      .0      .0
                              CONDENSATE WITH NAOH (PPM)    .0      .0      .0
                              CO2                           .0      .0      .0
                              H2S                           .0      .0      .0

IONIC STRENGTH =   .00816     IONIC BALANCE :   CATIONS (MOL.EQ.) .00632090
                                                ANIONS  (MOL.EQ.) .00700134
                                                DIFFERENCE  (%)    -10.22

DEEP WATER (PPM)                                DEEP STEAM (PPM)          GAS PRESSURES (BARS ABS.)

SIO2        73.32     CO2        119.58         CO2          .00          CO2        .497E-01
NA         139.46     H2S           .00         H2S          .00          H2S        .000E+00
K            2.49     H2            .00         H2           .00          H2         .000E+00
CA           4.29     O2            .00         O2           .00          O2         .000E+00
MG           .100     CH4           .00         CH4          .00          CH4        .000E+00
SO4        133.52     N2            .00         N2           .00          N2         .000E+00
CL          25.70     NH3           .00         NH3          .00          NH3        .000E+00
F           15.00                                                       H2O        .100E+02
DISS.S.    455.66                                                       TOTAL      .101E+02
AL           .1220
B            .1490                              H2O (%)                .00
FE           .0260                              BOILING PORTION        .00
```

ACTIVITY COEFFICIENTS IN DEEP WATER

H+	.885	KSO4-	.875	FE++	.593	FECL+	.870
OH-	.869	F-	.869	FE+++	.337	AL+++	.337
H3SIO4-	.870	CL-	.867	FEOH+	.874	ALOH++	.588
H2SIO4--	.588	NA+	.870	FE(OH)3-	.874	AL(OH)2+	.875
H2BO3-	.865	K+	.867	FE(OH)4--	.584	AL(OH)4-	.872
HCO3-	.870	CA++	.593	FEOH++	.584	ALSO4+	.872
CO3--	.580	MG++	.609	FE(OH)2+	.875	AL(SO4)2-	.872
HS-	.869	CAHCO3+	.877	FE(OH)4-	.875	ALF++	.588
S--	.584	MGHCO3+	.870	FESO4+	.874	ALF2+	.875
HSO4-	.872	CAOH+	.877	FECL++	.584	ALF4-	.872
SO4--	.576	MGOH+	.878	FECL2+	.874	ALF5--	.580
NASO4-	.875	NH4+	.865	FECL4-	.870	ALF6---	.294

CHEMICAL COMPONENTS IN DEEP WATER (PPM AND LOG MOLE)

H+ (ACT.)	.00	-7.706	MG++	.03	-5.943	FE(OH)3	.00	.000
OH-	4.12	-3.616	NACL	.11	-5.713	FE(OH)4-	.00	.000
H4SIO4	106.27	-2.956	KCL	.00	-8.006	FECL+	.00	-10.050
H3SIO4-	10.22	-3.969	NASO4-	6.43	-4.268	FECL2	.00	-18.389
H2SIO4--	.01	-7.112	KSO4-	.39	-5.538	FECL++	.00	.000
NAH3SIO4	.82	-5.159	CASO4	3.73	-4.563	FECL2+	.00	.000
H3BO3	.80	-4.889	MGSO4	.32	-5.580	FECL3	.00	.000
H2BO3-	.05	-6.064	CACO3	.97	-5.013	FECL4-	.00	.000
H2CO3	21.41	-3.462	MGCO3	.00	-7.486	FESO4	.00	-8.823
HCO3-	142.11	-2.633	CAHCO3+	2.84	-4.552	FESO4+	.00	.000
CO3--	.31	-5.286	MGHCO3+	.01	-7.113	AL+++	.00	-23.123
H2S	.00	.000	CAOH+	.04	-6.181	ALOH++	.00	-15.948
HS-	.00	.000	MGOH+	.01	-6.636	AL(OH)2+	.00	-9.466
S--	.00	.000	NH4OH	.00	.000	AL(OH)3	.20	-5.586
H2SO4	.00	-15.540	NH4+	.00	.000	AL(OH)4-	.18	-5.715
HSO4-	.02	-6.600	FE++	.00	-8.233	ALSO4+	.00	-22.328
SO4--	125.15	-2.885	FE+++	.00	.000	AL(SO4)2-	.00	-22.984
HF	.01	-6.225	FEOH+	.01	-6.782	ALF++	.00	-18.069
F-	14.99	-3.103	FE(OH)2	.02	-6.602	ALF2+	.00	-14.563
CL-	25.63	-3.141	FE(OH)3-	.00	-7.369	ALF3	.00	-13.019
NA+	138.01	-2.222	FE(OH)4--	.00	-11.769	ALF4-	.00	-13.354
K+	2.38	-4.216	FE(OH)++	.00	.000	ALF5--	.00	-14.906
CA++	1.65	-4.384	FE(OH)2+	.00	.000	ALF6---	.00	-17.752

IONIC STRENGTH = .00784 IONIC BALANCE : CATIONS (MOL.EQ.) .00617801
ANIONS (MOL.EQ.) .00680935
DIFFERENCE (%) -9.72

CHEMICAL GEOTHERMOMETERS DEGREES C 1000/T DEGREES KELVIN = 2.21

QUARTZ	110.3
CHALCEDONY	85.9
NAK	65.4

OXIDATION POTENTIAL (VOLTS) : EH H2S= 99.999 EH CH4= 99.999 EH H2= 99.999 EH NH3= 99.999

LOG SOLUBILITY PRODUCTS OF MINERALS IN DEEP WATER

	TEOR.	CALC.		TEOR.	CALC.		TEOR.	CALC.
ADULARIA	-15.061	-18.552	ALBITE LOW	-14.525	-16.555	ANALCIME	-11.803	-13.599
ANHYDRITE	-6.863	-7.737	CALCITE	-11.059	-10.134	CHALCEDONY	-2.320	-2.956
MG-CHLORITE	-80.826	-79.887	FLUORITE	-10.643	-10.940	GOETHITE	-1.316	99.999
LAUMONTITE	-24.819	-27.245	MICROCLINE	-15.982	-18.552	MAGNETITE	-23.293	99.999
CA-MONTMOR.	-74.275	-101.186	K-MONTMOR.	-35.282	-52.566	MG-MONTMOR.	-75.690	-102.733
NA-MONTMOR.	-35.486	-50.569	MUSCOVITE	-18.327	-22.006	PREHNITE	-35.860	-36.254
PYRRHOTITE	-59.075	99.999	PYRITE	-90.579	99.999	QUARTZ	-2.479	-2.956
WAIRAKITE	-23.816	-27.245	WOLLASTONITE	8.794	7.845	ZOISITE	-35.736	-37.982
EPIDOTE	-38.037	99.999	MARCASITE	-71.229	99.999			

UNU Geothermal Training Programme DEEP WATER COOLED TO 100.0 DEGREES C.
SAMPLE = 851115S-14

ACTIVITY COEFFICIENTS IN DEEP WATER

H+	.907	KSO4-	.899	FE++	.659	FECL+	.895
OH-	.894	F-	.894	FE+++	.419	AL+++	.419
H3SIO4-	.895	CL-	.892	FEOH+	.898	ALOH++	.654
H2SIO4--	.654	NA+	.895	FE(OH)3-	.898	AL(OH)2+	.899
H2BO3-	.891	K+	.892	FE(OH)4--	.651	AL(OH)4-	.897
HCO3-	.895	CA++	.659	FEOH++	.651	ALSO4+	.897
CO3--	.648	MG++	.672	FE(OH)2+	.899	AL(SO4)2-	.897
HS-	.894	CAHCO3+	.900	FE(OH)4-	.899	ALF++	.654
S--	.651	MGHCO3+	.895	FESO4+	.898	ALF2+	.899
HSO4-	.897	CAOH+	.900	FECL++	.651	ALF4-	.897
SO4--	.644	MGOH+	.902	FECL2+	.898	ALF5--	.648
NASO4-	.899	NH4+	.891	FECL4-	.895	ALF6---	.377

CHEMICAL COMPONENTS IN DEEP WATER (PPM AND LOG MOLE)

H+ (ACT.)	.00	-7.741	MG++	.06	-5.626	FE(OH)3	.00	.000
OH-	.58	-4.470	NACL	.04	-6.115	FE(OH)4-	.00	.000
H4SIO4	109.60	-2.943	KCL	.00	-8.504	FECL+	.00	-9.361
H3SIO4-	7.16	-4.124	NASO4-	2.68	-4.647	FECL2	.00	-22.931
H2SIO4--	.01	-7.238	KSO4-	.15	-5.965	FECL++	.00	.000
NAH3SIO4	.54	-5.339	CASO4	1.92	-4.850	FECL2+	.00	.000
H3BO3	.80	-4.890	MGSO4	.19	-5.797	FECL3	.00	.000
H2BO3-	.06	-6.040	CACO3	.47	-5.330	FECL4-	.00	.000
H2CO3	6.60	-3.973	MGCO3	.00	-7.363	FESO4	.00	-7.615
HCO3-	157.47	-2.588	CAHCO3+	1.08	-4.971	FESO4+	.00	.000
CO3--	.87	-4.839	MGHCO3+	.01	-7.060	AL+++	.00	-18.909
H2S	.00	.000	CAOH+	.00	-7.186	ALOH++	.00	-13.798
HS-	.00	.000	MGOH+	.00	-7.682	AL(OH)2+	.00	-9.222
S--	.00	.000	NH4OH	.00	.000	AL(OH)3	.05	-6.193
H2SO4	.00	-17.476	NH4+	.00	.000	AL(OH)4-	.37	-5.411
HSO4-	.00	-7.766	FE++	.01	-6.768	ALSO4+	.00	-18.754
SO4--	129.73	-2.869	FE+++	.00	.000	AL(SO4)2-	.00	-19.711
HF	.00	-7.054	FEOH+	.02	-6.587	ALF++	.00	-14.808
F-	15.00	-3.103	FE(OH)2	.00	-7.940	ALF2+	.00	-12.087
CL-	25.67	-3.140	FE(OH)3-	.00	-10.626	ALF3	.00	-11.030
NA+	138.82	-2.219	FE(OH)4--	.00	-15.632	ALF4-	.00	-11.649
K+	2.45	-4.203	FE(OH)++	.00	.000	ALF5--	.00	-13.316
CA++	3.11	-4.111	FE(OH)2+	.00	.000	ALF6---	.00	-15.981

IONIC STRENGTH = .00805 IONIC BALANCE : CATIONS (MOL.EQ.) .00627197
ANIONS (MOL.EQ.) .00693842
DIFFERENCE (%) -10.09

OXIDATION POTENTIAL (VOLTS) : EH H2S= 99.999 EH CH4= 99.999 EH H2= 99.999 EH NH3= 99.999

LOG SOLUBILITY PRODUCTS OF MINERALS IN DEEP WATER

	TEOR.	CALC.		TEOR.	CALC.		TEOR.	CALC.
ADULARIA	-17.222	-18.474	ALBITE LOW	-16.485	-16.488	ANALCIME	-13.199	-13.545
ANHYDRITE	-5.607	-7.353	CALCITE	-9.438	-9.320	CHALCEDONY	-2.841	-2.943
MG-CHLORITE	-80.302	-84.753	FLUORITE	-10.538	-10.595	GOETHITE	-4.674	99.999
LAUMONTITE	-27.182	-26.848	MICROCLINE	-18.598	-18.474	MAGNETITE	-29.703	99.999
CA-MONTMOR.	-85.559	-90.309	K-MONTMOR.	-41.648	-47.261	MG-MONTMOR.	-86.708	-91.816
NA-MONTMOR.	-41.660	-45.276	MUSCOVITE	-21.151	-20.222	PREHNITE	-36.778	-37.234
PYRRHOTITE	-99.806	99.999	PYRITE	-147.012	99.999	QUARTZ	-3.098	-2.943
WAIRAKITE	-24.710	-26.848	WOLLASTONITE	10.824	8.246	ZOISITE	-35.893	-38.108
EPIDOTE	-43.603	99.999	MARCASITE	-123.575	99.999			

DEEP WATER COOLED TO 20.0 DEGREES C.

ACTIVITY COEFFICIENTS IN DEEP WATER

H+	.919	KSO4-	.912	FE++	.698	FECL+	.909
OH-	.908	F-	.908	FE+++	.472	AL+++	.472
H3SIO4-	.909	CL-	.907	FEOH+	.912	ALOH++	.695
H2SIO4--	.695	NA+	.909	FE(OH)3-	.912	AL(OH)2+	.912
H2RO3-	.906	K+	.907	FE(OH)4--	.692	AL(OH)4-	.910
HCO3-	.909	CA++	.698	FEOH++	.692	ALSO4+	.910
CO3--	.689	MG++	.710	FE(OH)2+	.912	AL(SO4)2-	.910
HS-	.908	CAHCO3+	.914	FE(OH)4-	.912	ALF++	.695
S--	.692	MGHCO3+	.909	FESO4+	.912	ALF2+	.912
HSO4-	.910	CAOH+	.914	FECL++	.692	ALF4-	.910
SO4--	.685	MGOH+	.915	FECL2+	.912	ALF5--	.689
NASO4-	.912	NH4+	.906	FECL4-	.909	ALF6---	.432

CHEMICAL COMPONENTS IN DEEP WATER (PPM AND LOG MOLE)

H+ (ACT.)	.00	-8.298	MG++	.09	-5.444	FE(OH)3	.00	.000
OH-	.03	-5.818	NACL	.01	-7.043	FE(OH)4-	.00	.000
H4SIO4	114.68	-2.923	KCL	.00	-8.988	FECL+	.00	-10.180
H3SIO4-	2.40	-4.598	NASO4-	1.08	-5.043	FECL2	.00	-31.670
H2SIO4--	.00	-8.002	KSO4-	.05	-6.420	FECL++	.00	.000
NAH3SIO4	.21	-5.746	CASO4	.88	-5.187	FECL2+	.00	.000
H3RO3	.77	-4.905	MGSO4	.05	-6.409	FECL3	.00	.000
H2RO3-	.08	-5.875	CACO3	.16	-5.792	FECL4-	.00	.000
H2CO3	1.96	-4.501	MGCO3	.00	-7.352	FESO4	.01	-7.382
HCO3-	161.96	-2.576	CAHCO3+	.16	-5.793	FESO4+	.00	.000
CO3--	1.68	-4.554	MGHCO3+	.01	-7.113	AL+++	.00	-14.748
H2S	.00	.000	CAOH+	.00	-8.790	ALOH++	.00	-11.525
HS-	.00	.000	MGOH+	.00	-9.245	AL(OH)2+	.00	-8.706
S--	.00	.000	NH4OH	.00	.000	AL(OH)3	.03	-6.413
H2SO4	.00	-20.737	NH4+	.00	.000	AL(OH)4-	.39	-5.385
HSO4-	.00	-9.343	FE++	.02	-6.393	ALSO4+	.00	-15.077
SO4--	131.94	-2.862	FE+++	.00	.000	AL(SO4)2-	.00	-16.222
HF	.00	-8.302	FEOH+	.00	-7.707	ALF++	.00	-11.102
F-	15.00	-3.103	FE(OH)2	.00	-10.891	ALF2+	.00	-8.765
CL-	25.69	-3.140	FE(OH)3-	.00	-15.933	ALF3	.00	-7.901
NA+	139.21	-2.218	FE(OH)4--	.00	-22.058	ALF4-	.00	-8.624
K+	2.47	-4.199	FE(OH)++	.00	.000	ALF5--	.00	-10.293
CA++	3.90	-4.012	FE(OH)2+	.00	.000	ALF6---	.00	-12.716

IONIC STRENGTH = .00816 IONIC BALANCE : CATIONS (MOL.EQ.) .00632282
ANIONS (MOL.EQ.) .00700387
DIFFERENCE (%) -10.22

OXIDATION POTENTIAL (VOLTS) : EH H2S= 99.999 EH CH4= 99.999 EH H2= 99.999 EH NH3= 99.999

LOG SOLUBILITY PRODUCTS OF MINERALS IN DEEP WATER

	TEOR.	CALC.		TEOR.	CALC.		TEOR.	CALC.
ADULARIA	-21.669	-18.396	ALBITE LOW	-20.545	-16.415	ANALCIME	-16.278	-13.491
ANHYDRITE	-4.665	-7.194	CALCITE	-8.457	-8.883	CHALCEDONY	-3.646	-2.923
MG-CHLORITE	-85.790	-94.379	FLUORITE	-11.026	-10.457	GOETHITE	-7.464	99.999
LAUMONTITE	-32.762	-26.632	MICROCLINE	-23.747	-18.396	MAGNETITE	-36.123	99.999
CA-MONTMOR.	-113.523	-73.562	K-MONTMOR.	-56.733	-38.938	MG-MONTMOR.	-114.120	-74.986
NA-MONTMOR.	-56.347	-36.956	MUSCOVITE	-28.029	-17.448	PREHNITE	-41.653	-39.596
PYRRHOTITE	-140.994	99.999	PYRITE	-212.014	99.999	QUARTZ	-4.055	-2.923
WAIRAKITE	-28.204	-26.632	WOLLASTONITE	13.966	9.506	ZOISITE	-40.005	-39.122
EPIDOTE	-50.882	99.999	MARCASITE	-182.235	99.999			

Appendix II. An example of data used for log(Q/K) diagram construction.

SINO-9, WELL18

	MINERALS	TEMPERATURES				
	LOG(Q/K)\ T°C		20	40	60	80
1	ADULARIA	1	5.107	3.712	2.51	1.479
2	ANHYDRITE	2	-0.594	-0.447	-0.285	-0.117
3	CA-MONTMOR	5	65.629	51.228	38.255	27.04
4	NA-MONTMOR	6	32.159	24.759	18.093	12.321
5	WAIRAKITE	8	4.428	3.246	2.256	1.445
6	ALBITE LOW	10	5.597	4.325	3.226	2.283
7	CALCITE	11	-0.634	-0.476	-0.306	-0.132
8	MICROCLINE	13	7.185	5.588	4.202	3.005
9	K-MONTMOR	14	30.93	23.396	16.625	10.766
10	PYRITE	16	36.95	27.742	19.519	12.253
11	MARCASITE	18	7.171	-0.139	-6.698	-12.494
12	ANALCIME	19	4.149	3.177	2.338	1.621
13	CHALCEDONY	20	0.827	0.587	0.376	0.188
14	GOETHITE	21	-1.421	-0.812	-0.264	0.231
15	MAGNETITE	22	-1.575	0.287	1.97	3.502
16	MG-MONTMOR	23	64.347	50.117	37.287	26.192
17	QUARTZ	25	1.236	0.951	0.7	0.477

	MINERALS	TEMPERATURES				
	LOG(Q/K)\ T°C		100	120	140	160
1	ADULARIA	1	0.604	-0.134	-0.747	-1.249
2	ANHYDRITE	2	0.065	0.249	0.439	0.631
3	CA-MONTMOR	5	17.621	9.874	3.601	-1.429
4	NA-MONTMOR	6	7.461	3.448	0.181	-2.457
5	WAIRAKITE	8	0.803	0.319	-0.021	-0.23
6	ALBITE LOW	10	1.481	0.806	0.247	-0.208
7	CALCITE	11	0.038	0.207	0.375	0.545
8	MICROCLINE	13	1.98	1.108	0.375	-0.234
9	K-MONTMOR	14	5.835	1.762	-1.557	-4.24
10	PYRITE	16	5.844	0.156	-4.991	-10.298
11	MARCASITE	18	-17.593	-22.105	-26.189	-30.531
12	ANALCIME	19	1.016	0.513	0.102	-0.223
13	CHALCEDONY	20	0.02	-0.131	-0.267	-0.391
14	GOETHITE	21	0.681	1.087	1.447	1.692
15	MAGNETITE	22	4.9	6.174	7.319	8.148
16	MG-MONTMOR	23	16.875	9.213	3.012	-1.956
17	QUARTZ	25	0.277	0.099	-0.064	-0.211

Table 3.1 List of conventional geothermometers (from Fournier, 1981)

Geothermometer	Equation	Restrictions
a. Quartz-no steam loss	$t°C = \frac{1309}{5{\cdot}19 - \log C} - 273{\cdot}15$	$t = 0$–$250°C$
b. Quartz-maximum steam loss	$t°C = \frac{1522}{5{\cdot}75 - \log C} - 273{\cdot}15$	$t = 0$–$250°C$
c. Chalcedony	$t°C = \frac{1032}{4{\cdot}69 - \log C} - 273{\cdot}15$	$t = 0$–$250°C$
d. α-Cristobalite	$t°C = \frac{1000}{4{\cdot}78 - \log C} - 273{\cdot}15$	$t = 0$–$250°C$
e. β-Cristabalite	$t°C = \frac{781}{4{\cdot}51 - \log C} - 273{\cdot}15$	$t = 0 - 250°C$
f. Amorphous silica	$t°C = \frac{731}{4{\cdot}52 - \log C} - 273{\cdot}15$	$t = 0 - 250°C$
g. Na/K (Fournier)	$t°C = \frac{1217}{\log (Na/K) + 1{\cdot}483} - 273{\cdot}15$	$t > 150°C$
h. Na/K (Truesdell)	$t°C = \frac{855{\cdot}6}{\log (Na/K) + 0{\cdot}8573} - 273{\cdot}15$	$t > 150°C$
i. Na–K–Ca	$t°C = \frac{1647}{\log (Na/K) + \beta[\log(\sqrt{Ca}/Na) + 2{\cdot}06] + 2{\cdot}47} - 273{\cdot}15$	$t < 100°C$, $\beta = 4/3$ $t > 100°C$, $\beta = 1/3$
j. $\Delta^{18}O(SO_4^{=} - H_2O)$	$1000 \ln \alpha = 2{\cdot}88(10^6 T^{-2}) - 4{\cdot}1$ $\alpha = \frac{1000 + \delta^{18}O(HSO_4^-)}{1000 + \delta^{18}O(H_2O)}$ and $T = °K$	

Table 3.2 Free energies of formation of minerals and aqueous species in kJ/mole at the saturated vapor pressure of pure water (from Helgeson et al., 1978)

	Temperature (°C)					
	100	150	200	250	300	350
Quartz	-859.8	-862.7	-865.7	-869.0	-872.4	-876.5
Albite	-3725.9	-3739.3	-3754.3	-3770.6	-3787.8	-3805.8
K-feldspar	-3763.9	-3777.7	-3793.2	-3810.0	-3827.5	-3845.9
Muscovite	-5615.8	-5639.2	-5656.8	-5680.6	-5706.1	-5732.9
Kaolinite	-3806.6	-3820.4	-3836.3	-3853.5	-3872.3	-3892.4
Calcite	-1137.6	-1143.9	-1150.2	-1157.3	-1164.4	-1172.4
Wairakite	-6215.8	-6235.0	-6274.7	-6307.4	-6342.5	-6378.9
Zoisite	-6515.3	-6534.6	-6556.3	-6580.2	-6606.1	-6633.7
H^+	0	0	0	0	0	0
Na^+	-266.9	-270.7	-274.9	-279.1	-283.7	-286.2
K^+	-290.4	-295.8	-301.7	-307.5	-312.5	-317.6
Ca^{++}	-548.9	-546.0	-543.5	-540.6	-535.6	-523.8
H_2O liquid	-243.1	-247.7	-252.7	-258.2	-264.0	-269.9
H_2O vapor	-243.1	-253.1	-263.2	-273.2	-284.1	-294.6
CO_2, gas	-410.9	-422.2	-433.5	-445.2	-457.3	-469.4

Table 5.1. Equilibrium constants for minerals used in the WATCH program (from Arnorsson et al., 1982)

	MINERAL	REACTION	TEMPERATURE FUNCTION (°K)
401	ADULARIA	$KAlSi_3O_8 + 8H_2O = K^+ + Al(OH)_4^- + 3H_4SiO_4^o$	+38.85 −0.0458T −17260/T +1012722/T^2
402	LOW-ALBITE	$NaAlSi_3O_8 + 8H_2O = Na^+ + Al(OH)_4^- + 3H_4SiO_4^o$	+36.83 −0.0439T −16474/T +1004631/T^2
403	ANALCIME	$NaAlSi_2O_6{\cdot}H_2O + 5H_2O = Na^+ + Al(OH)_4^- + 2H_4SiO_4^o$	+34.08 −0.0407T −14577/T +970981/T^2
404	ANHYDRITE	$CaSO_4 = Ca^{+2} + SO_4^{-2}$	+6.20 −0.0229T −1217/T
405	CALCITE	$CaCO_3 = Ca^{+2} + CO_3^{-2}$	+10.22 −0.0349T −2476/T
406	CHALCEDONY	$SiO_2 + 2H_2O = H_4SiO_4^o$	+0.11 −1101/T
407	Mg-CHLORITE	$Mg_5Al_2Si_3O_{10}(OH)_8 + 10H_2O = 5Mg^{+2} + Al(OH)_4^- + 3H_4SiO_4^o + 8OH^-$	−1022.12 −0.3861T +9363/T +412.461ogT
408	FLUORITE	$CaF_2 = Ca^{+2} + 2F^-$	+66.54 −4318/T −25.471ogT
409	GOETHITE	$FeOOH + H_2O + OH^- = Fe(OH)_4^-$	−80.34 +0.099T +20290/T −2179296/T^2
410	LAUMONTITE	$CaAl_2Si_4O_{12}{\cdot}4H_2O + 8H_2O = Ca^{+2} + 2Al(OH)_4^- + 4H_4SiO_4^o$	+65.95 −0.0828T −28358/T +1916098/T^2
411	MICROCLINE	$KAlSi_3O_8 + 8H_2O = K^+ + Al(OH)_4^- + 3H_4SiO_4^o$	+44.55 −0.0498T −19883/T +1214019/T^2
412	MAGNETITE	$Fe_3O_4 + 4H_2O = 2Fe(OH)_4^- + Fe^{+2}$	−155.58 +0.1658T +35298/T −4258774/T^2
413	Ca-MONTMOR.	$6Ca_{0.167}Al_{2.33}Si_{3.67}O_{10}(OH)_2 + 6OH_2O + 12OH^- = Ca^{+2} + 14Al(OH)_4^- + 22H_4SiO_4^o$	+30499.49 +3.5109T −1954295/T +125536640/T^2 −10715.661ogT
414	K-MONTMOR.	$3K_{0.33}Al_{2.33}Si_{3.67}O_{10}(OH)_2 + 30H_2O + 6OH^- = K^+ + 7Al(OH)_4^- + 11H_4SiO_4^o$	+15075.11 +1.7346T −967127/T +61985927/T^2 −5294.721ogT
415	Mg-MONTMOR.	$6Mg_{0.167}Al_{2.33}Si_{3.67}O_{10}(OH)_2 + 6OH_2O + 12OH^- = Mg^{+2} + 14Al(OH)_4^- + 22H_4SiO_4^o$	+30514.87 +3.5188T −1953843/T +125538830/T^2 −10723.711ogT
416	Na-MONTMOR.	$3Na_{0.33}Al_{2.33}Si_{3.67}O_{10}(OH)_2 + 30H_2O + 6OH^- = Na^+ + 7Al(OH)_4^- + 11H_4SiO_4^o$	+15273.90 +1.7623T −978782/T +62805036/T^2 −5366.181ogT
417	MUSCOVITE	$KAl_3Si_3O_{10}(OH)_2 + 10H_2O + 2OH^- = K^+ + 3Al(OH)_4^- + 3H_4SiO_4^o$	+6113.68 +0.6914T −394755/T +25226323/T^2 −2144.771ogT
418	PREHNITE	$Ca_2Al_2Si_3O_{10}(OH)_2 + 10H_2O = 2Ca^{+2} + 2Al(OH)_4^- + 2OH^- + 3H_4SiO_4^o$	+90.53 −0.1298T −36162/T +2511432/T^2
419	PYRRHOTITE	$8FeS + SO_4^{-2} + 22H_2O + 6OH^- = 8Fe(OH)_4^- + 9H_2S$	+3014.68 +1.2522T −103450/T −1284.861ogT
420	PYRITE	$8FeS_2 + 26H_2O + 10OH^- = 8Fe(OH)_4^- + SO_4^{-2} + 15H_2S$	+4523.89 +1.6002T −180405/T −1860.331ogT
421	QUARTZ	$SiO_2 + 2H_2O = H_4SiO_4^o$	+0.41 −1309/T (0–250°C); +0.12 −1164/T (180–300°C)
422	WAIRAKITE	$CaAl_2Si_4O_{12}{\cdot}2H_2O + 10H_2O = Ca^{+2} + 2Al(OH)_4^- + 4H_4SiO_4^o$	+61.00 −0.0847T −25018/T +1801911/T^2
423	WOLLASTONITE	$CaSiO_3 + 2H^+ + H_2O = Ca^{+2} + H_4SiO_4^o$	−222.85 −0.0337T +16258/T −671106/T^2 +80.681ogT
424	ZOISITE	$Ca_2Al_3Si_3O_{12}(OH) + 12H_2O = 2Ca^{+2} + 3Al(OH)_4^- + 3H_4SiO_4^o + OH^-$	+106.61 −0.1497T −40448/T +3028977/T^2
425	EPIDOTE	$Ca_2FeAl_2Si_3O_{12}(OH) + 12H_2O = 2Ca^{+2} + Fe(OH)_4^- + 2Al(OH)_4^- + 3H_4SiO_4^o + OH^-$	−27399.84 −3.8749T +1542767/T −92778364/T^2 +9850.381ogT
426	MARCASITE	$8FeS_2 + 26H_2O + 10OH^- = 8Fe(OH)_4^- + SO_4^{-2} + 15H_2S$	+4467.61 +1.5879T −169944/T −1838.451ogT

Table 5.2. Classification of log(Q/K) curves by their slope as they appear in the diagrams and chemical composition of the minerals (see Figure 5.5).

GROUP	MINERAL(S)	CHEMICAL COMPOSITION
1.	MG-MONTMOR.	$Mg_{0.33}Al_2Si_4O_{10}(OH)_2 \cdot nH_2O$
	CA-MONTMOR.	$Ca_{0.33}Al_2Si_4O_{10}(OH)_2 \cdot nH_2O$
	NA-MONTMOR.	$Na_{0.33}Al_2Si_4O_{10}(OH)_2 \cdot nH_2O$
	K-MONTMOR.	$K_{0.33}Al_2Si_4O_{10}(OH)_2 \cdot nH_2O$
2.	MUSCOVITE	$KAl_2(AlSi_3)O_{10}(OH)_2$
	LAUMONITE	$CaAl_2Si_4O_{12} \cdot 4H_2O$
	MICROCLINE	$KAlSi_3O_8$
	ALBITE LOW	$NaAlSi_3O_8$
	ADULARIA	$KAlSi_3O_8$
	ANALCIME	$NaAlSi_2O_6 \cdot H_2O$
	PREHNITE	$Ca_2Al_2Si_3O_{10}(OH)_2$
	WAIRAKITE	$CaAl_2Si_4O_{12} \cdot 2H_2O$
	ZOISITE	$Ca_2Al_2Si_3O_{12}(OH)$
3.	QUARTZ	SiO_2
	CHALCEDONY	SiO_2
	FLUORITE	CaF_2
4.	CALCITE	$CaCO_3$
	ANHYDRITE	$CaSO_4$
	WOLLASTONITE	$CaSiO_3$
5.	MG-CHLORITE	$Mg_6AlSi_3O_{10}(OH)_8$
MINERALS OUT OF SCALE		
	PYRRHOTITE	$Fe_{1-x}S$
	EPIDOTE	$Ca_2(Al,Fe)_3Si_3O_{12}(OH)$
	MARSCASITE	FeS_2
	PYRITE	FeS_2
	GOETHITE	$_aFeO(OH)$
	MAGNETITE	$(Fe,Mg)Fe_2O_4$

Table 7.1 Summary of results for the Icelandic samples

Sample Number and Location	Equilibria Conditions	Temperatures °C						
		Sampling	Locus	Equilibrium	Reservoir	Chalcedony	Quartz	NaK
16, Reykir, well 17	No*	76	50 - 95		75 - 81	65	91	78
18, Reykjavik, well 30	No (boiling)	100	93 - 110		93 - 110	90	114	119
20, Seltjarnarnes, well 4	No (boiling)	114	30 - 100		119 - 126	112	135	91
20-1, well 2, 80 meter depth	No (dilution)*	Nm	65 - 100		119 - 126	61	86	52
20-2, well 2, 570 meter depth	Yes	Nm	95 - 130	110	119 - 126	102	125	82
20-3, well 2, 725 meter depth	Yes	Nm	95 - 135	130	119 - 126	98	122	69
21, Reykir, Lundareykjad., spring	No (dilution)*	75	60 - 140		?	130	152	110
21-1, Thvera, cold spring	No (dilution)	3.6	45 - 80		Ambient	24	49	112
21-2, England, hot spring	No* 140	91	70 - 140		95	130	152	104
39, Saudarkrokur, well 1	No*	68	40 - 110		70	79	103	67
50, Urridavatn, well 3	No (dilution)*	39	30 - 80		59	52	78	54
50-1, well 8	No (dilution)	77	40 - 100		77	77	102	65
50-2, well 4	No (dilution)	60	30 - 90		65	68	93	57
55, Leira, well 4	Yes	128	150 - 190	164	134 - 173	162	183	214
60, Reykjanes, Isafjardard., spring	No (dilution)	84	40 - 100		96	86	110	82
60-1, hot spring 11 - 301	Yes	78.8	72 - 120	85	96	91	115	94
60-2, hot spring 11 - 302	No (dilution)*	94	50 - 110		96	94	118	71
60-3, hot spring 11 - 306	No (dilution)*	84	50 - 110		96	91	115	72
61, Gjogur, spring	Yes	72	60 - 95	77	?	71	96	82
63, Lysuholl, well 6	No (dilution)	60	105 - 160		63	141	163	171
IRDP, Areyjar	No	42.8	30 - 160		47 - 78	74	51	99

Notes: 1.The sample numbers are the same as in Arnorsson's paper (1983a), but the ones followed by dashes are samples taken by the National Energy Authority from the same areas or very close to the locations marked in Figure 6.1;
2.The ones marked with * are those with very widely dispersed clay minerals in their log(Q/K) diagrams;

Table 7.2 Summary of results for the Chinese samples

Sample Number and Location	Equilibria Conditions	Temperatures ° C						
		Sampling	Locus	Equilibrium	Reservoir	Chalcedony	Quartz	NaK
1. Hot springs of western Zhanhzhou, no seawater influence								
1.1 Nanjin	Yes	78.5	70 - 115	90	90	86	111	66
1.2 Hua-an	No (dilution)	61.7	65 - 105			85	109	104
1.3 Xingtang	No (dilution)	35.4	50 - 85		50	81	105	70
2. Hot springs of western Zhangzhou, mixing with seawater					90 - 110			
2.1 Tang-an	No (contamination)	79.9	100 - 13			97	120	126
2.2 Xinlin	No (contamination)	93.3	100 - 170			103	126	90
2.3 Gangwei	No (contamination)	77.7	80 - 125			84	109	95
3. Geothermal well water from the Zhangzhou geothermal field					120 - 125			
3.1 Longsi	No (contamination)	98	110 - 175			113	146	145
3.2 Shuihuazan	No (contamination)	97.4	110 - 175			115	138	144
3.3 Xingjiangzaotang	Close (slight dilution)	37.2	85 - 140	117		83	108	182
3.4 Jucizan	No (contamination)	78.8	100 - 160			102	126	119
3.5 Sizhongyiyuan	No (contamination)	51.6	85 - 140			83	107	131
3.6 Xiazuang	No (contamination)	56.3	95 - 140			74	99	101

Notes: 1. Non-geothermal waters for which the calculations have been performed calculations on are not included in this table;
2. Inflow temperature (for wells) or the highest measured temperature (for hot springs) are used for the reference " reservior temperature in the table.

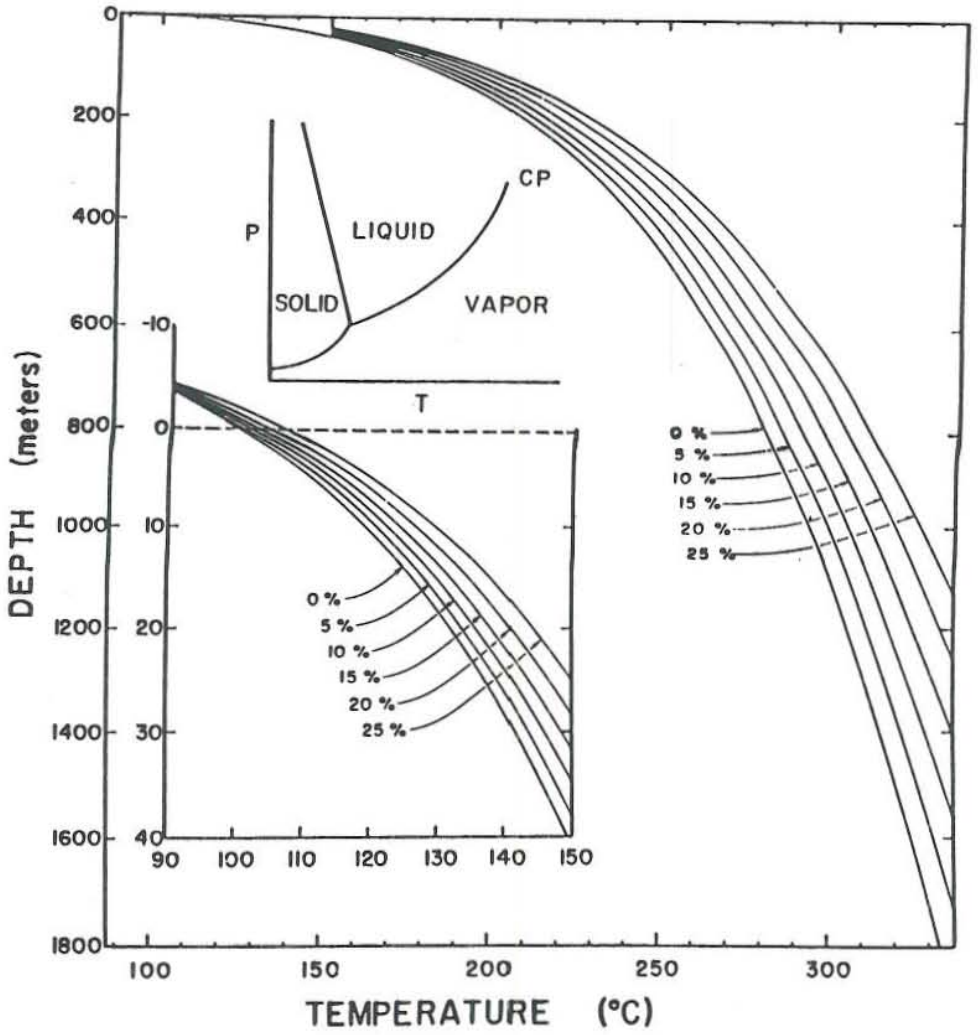

Figure 2.1. Boiling - point versus depth curves for waters with different wt% of NaCl compositions (from Haas, 1971).

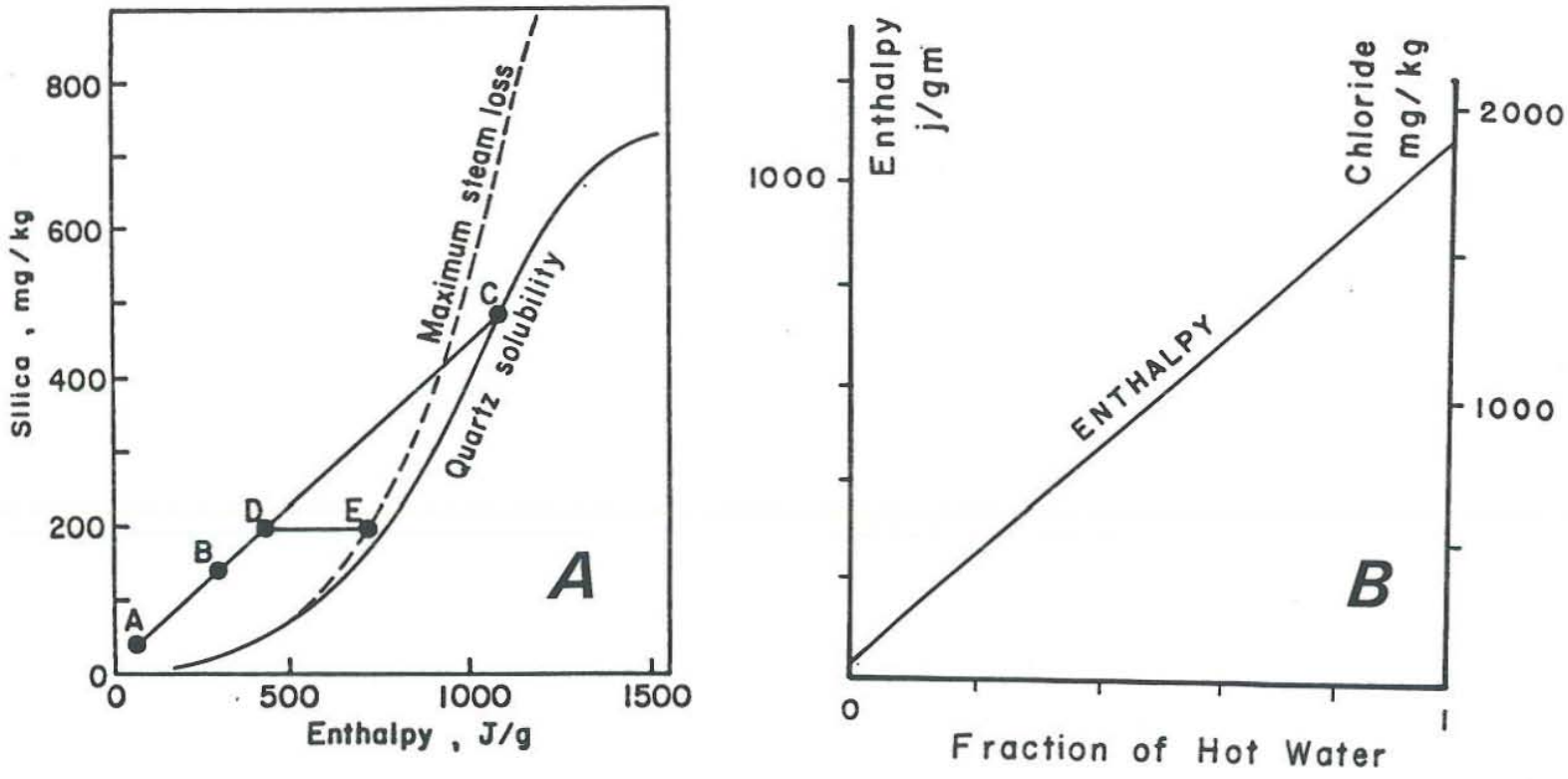

Figure 3.1. Mixing models using enthalpy balance assumption (from Fournier, 1981):
a) Silica mixing model;
b) Chloride mixing model.

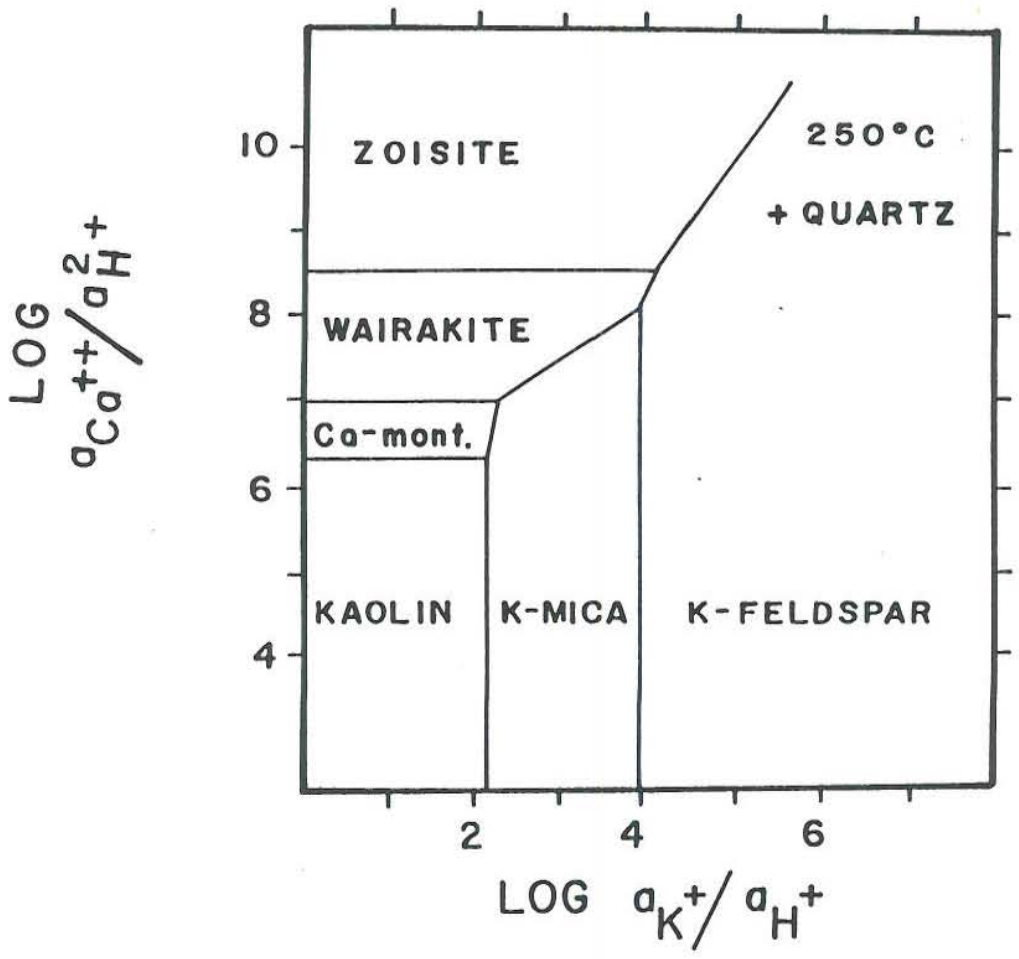

Figure 3.2. An example of an activity - activity diagram (from Henley, 1984b)

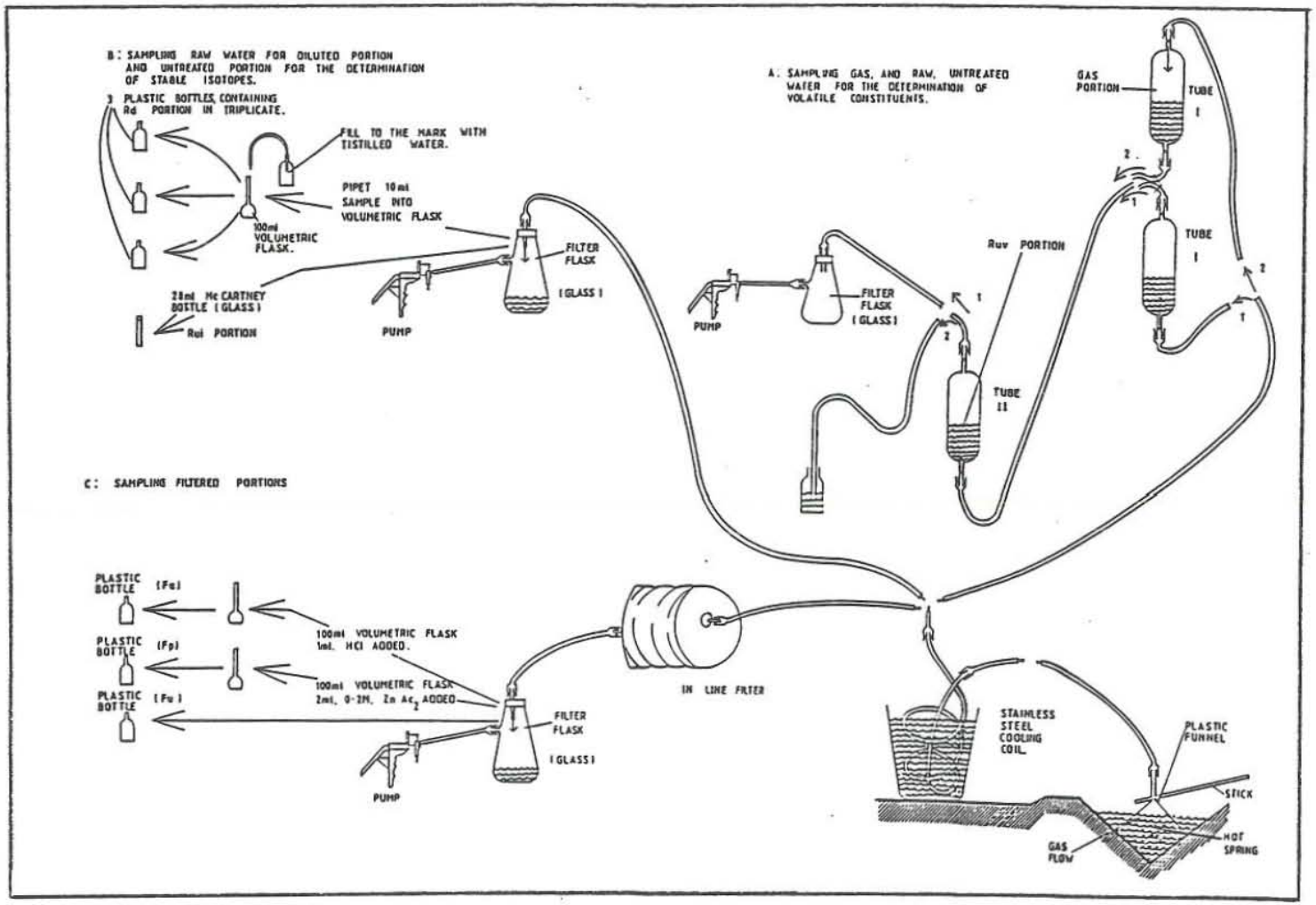

Figure 4.1. A drawing showing the method for sampling water and gas from hot springs.

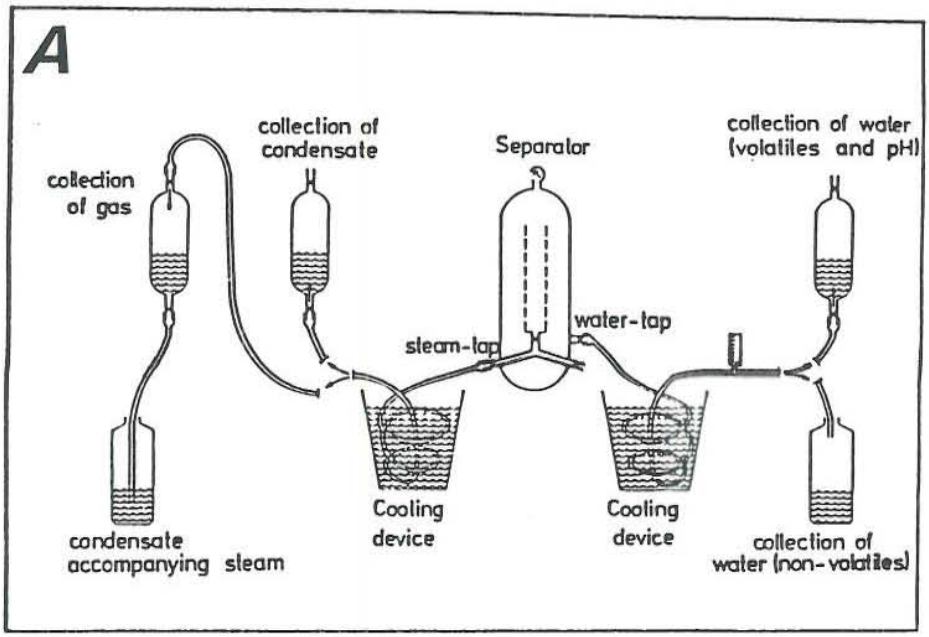

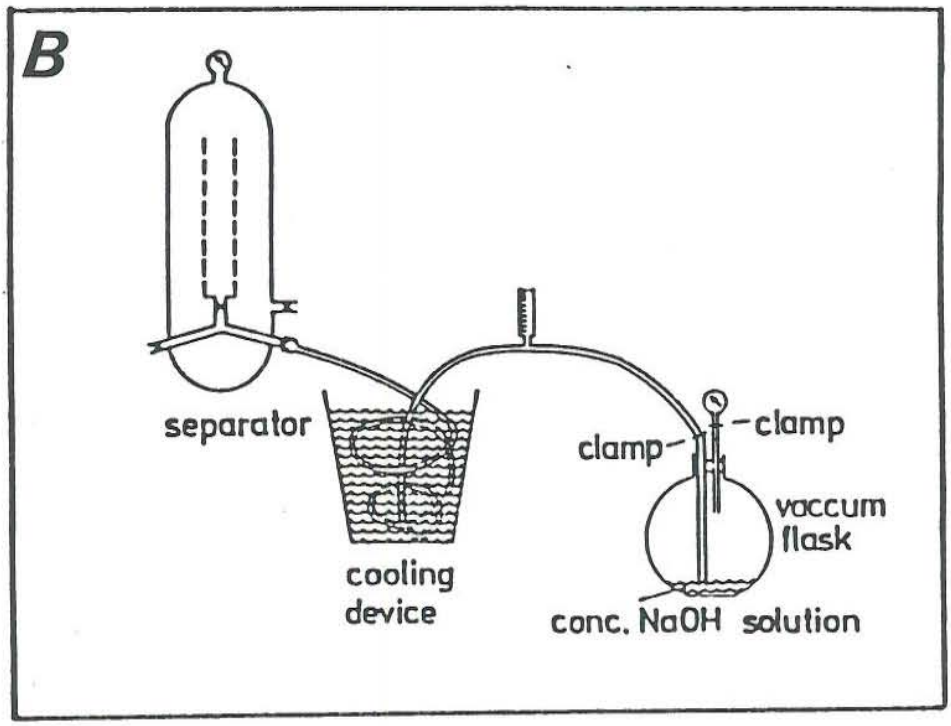

Figure 4.2. Schematic drawing showing the system for sampling from high temperature wells:

a) Collecting water, condensate and non-condensable gas fractions;

b) Collecting total steam.

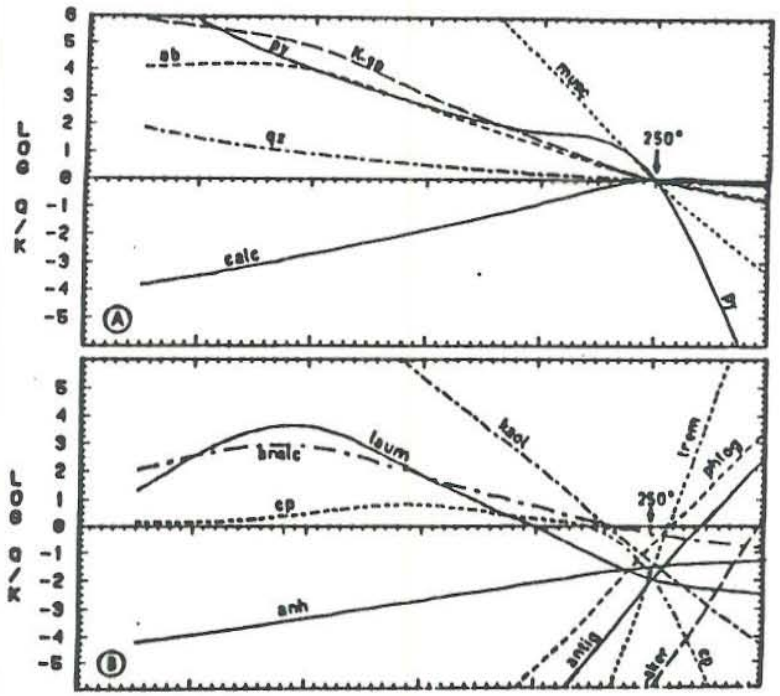

Figure 5.1. Theoretical model for log(Q/K) equilibria for a synthetic geothermal water that was arbitrarily equilibrated with muscovite, K-spar, pyrite, albite, quartz and calcite at 250°C by a heterogeneous equilibrium calculation (from Reed and Spycher, 1984) showing:

a) The curves for minerals that equilibrate cross the log(Q/K) = 0 line at the same given temperature;

b) Minerals that do not equilibrate do not conform with the theoretical equilibria.

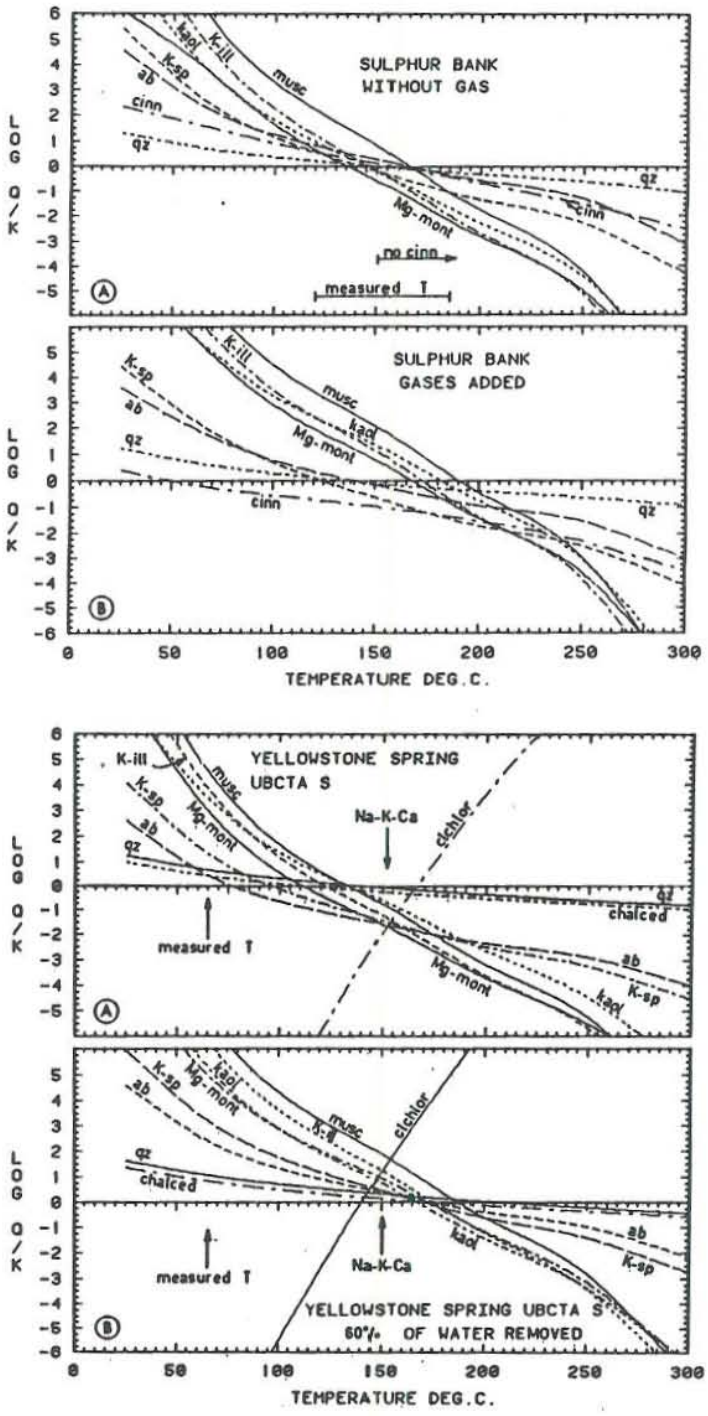

Figure 5.2. Examples showing the effects of boiling.

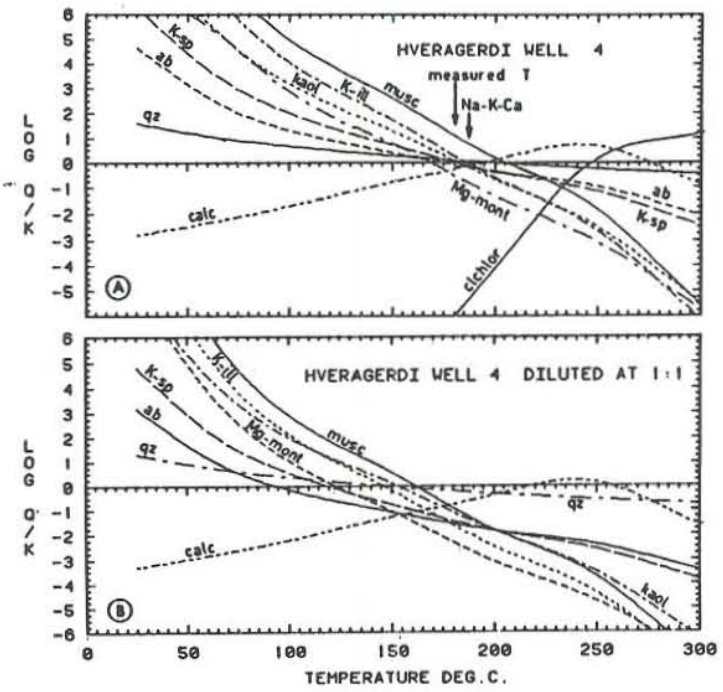

Figure 5.3 An example showing the effect of dilution.

Figure 5.4 Theoretical solubility (logK) curves from the WATCH program.

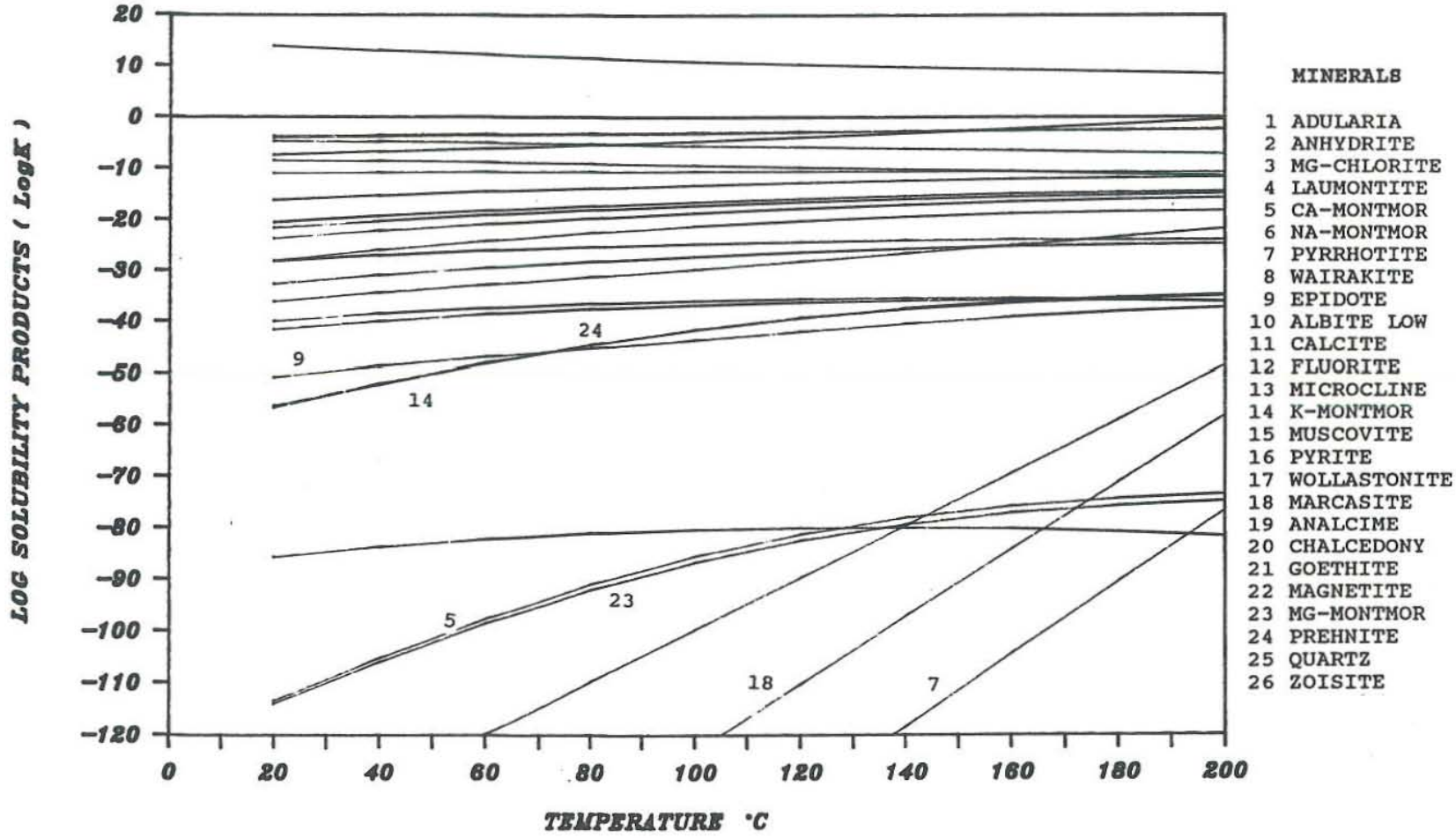

Figure 5.5 An example showing the log(Q/K) diagram for all minerals that stay within the selected temperature and log(Q/K) scale ranges.

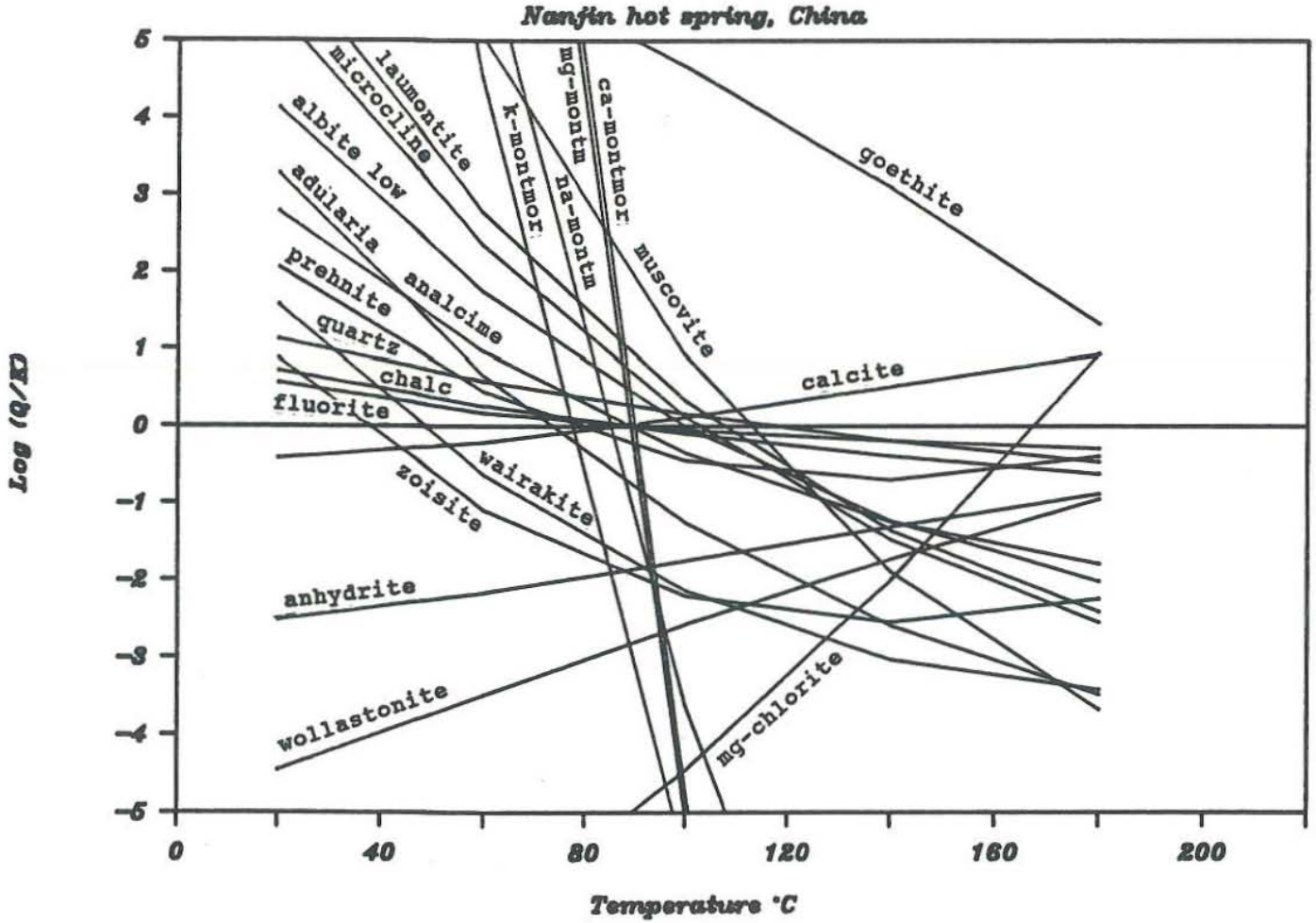

Figure 5.6 An example showing the distribution of possible equilibrium temperatures in the log(Q/K) diagram in a case of equilibrium.

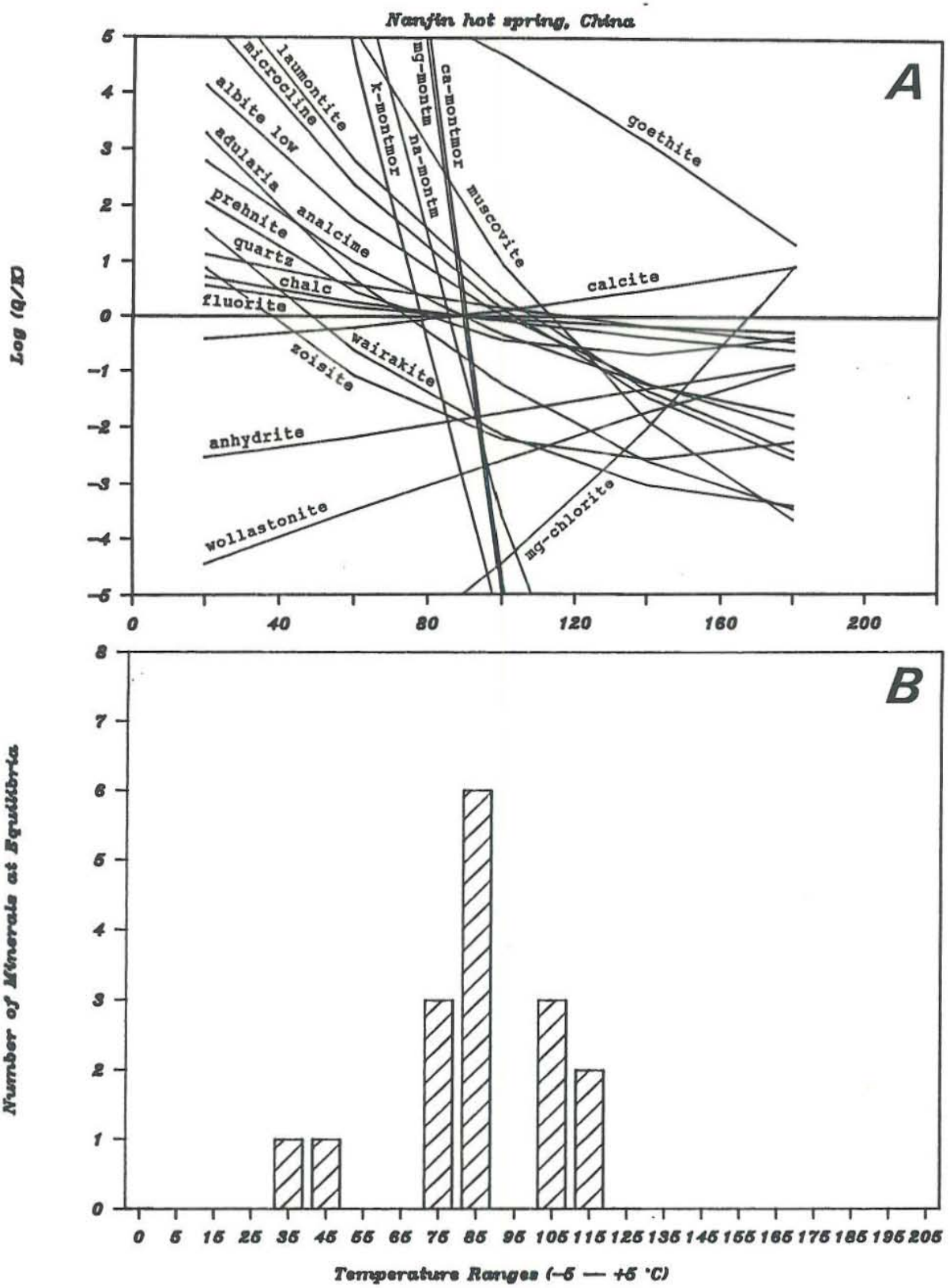

Figure 5.7 An example showing the distribution of possible equilibrium temperatures in the log(Q/K) diagram in a case of non-equilibrium.

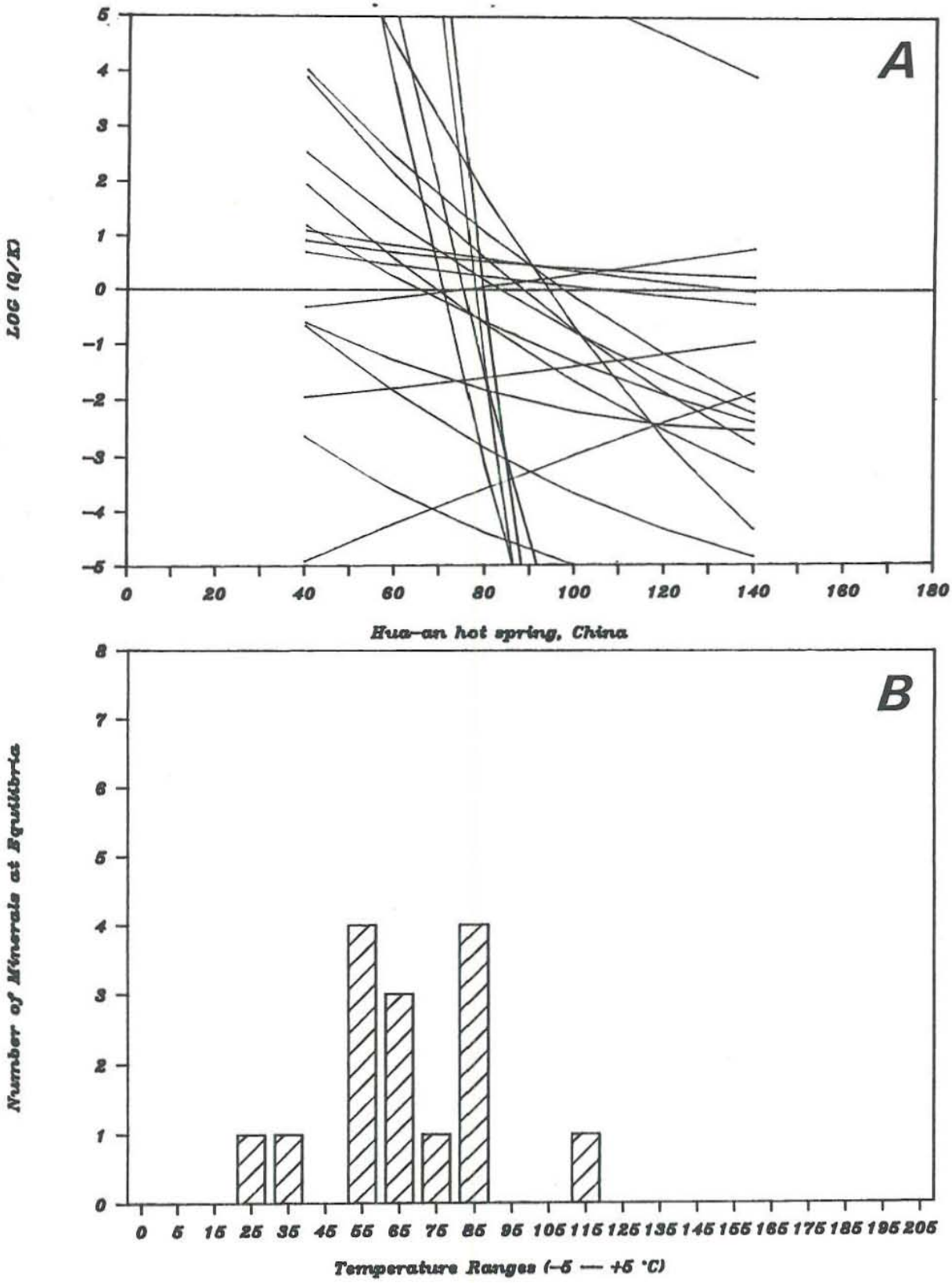

Figure 5.8 Log(Q/K) diagrams from WATCH showing the effect of dilution by mixing of relatively "pure" groundwater (1:1 ratio).

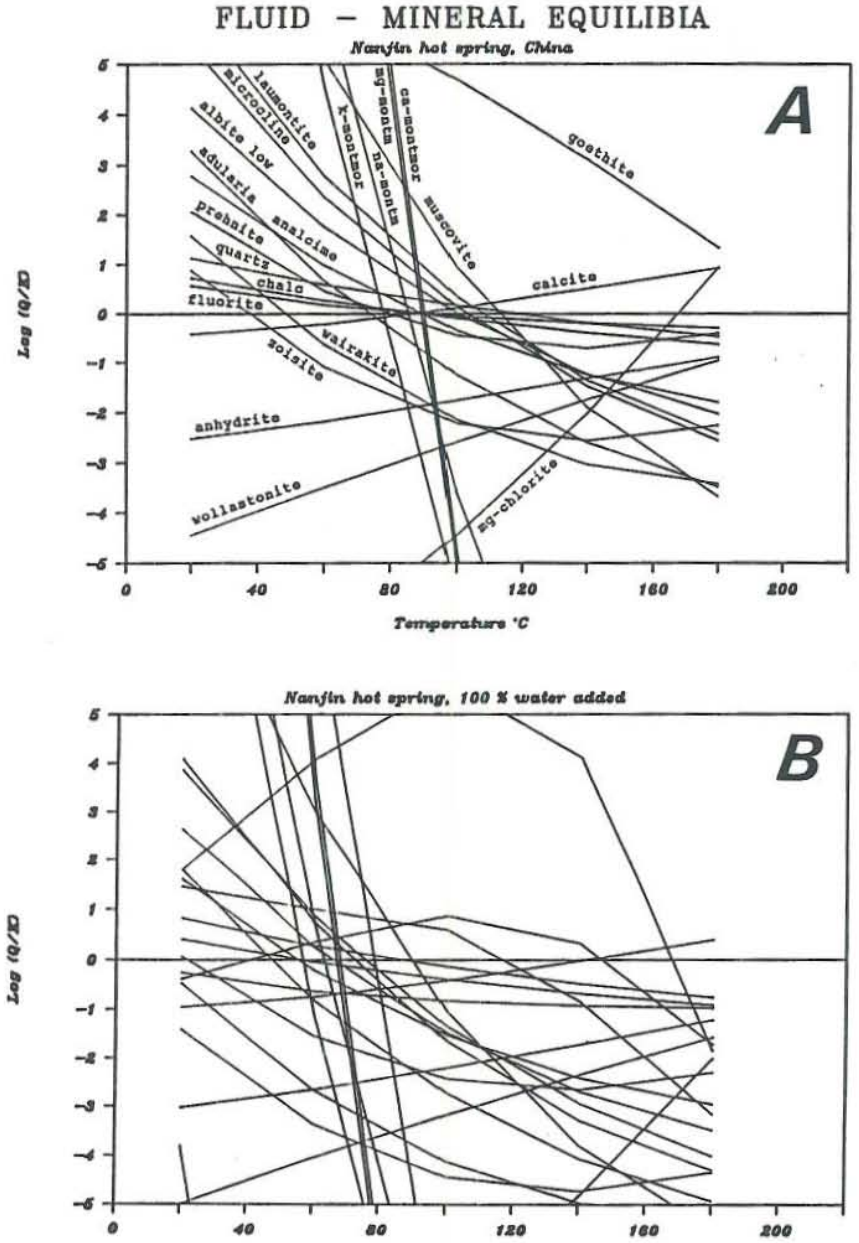

Figure 5.9 Log(Q/K) diagram from WATCH showing the effect of simple removal of water from the sample (simple steam loss).

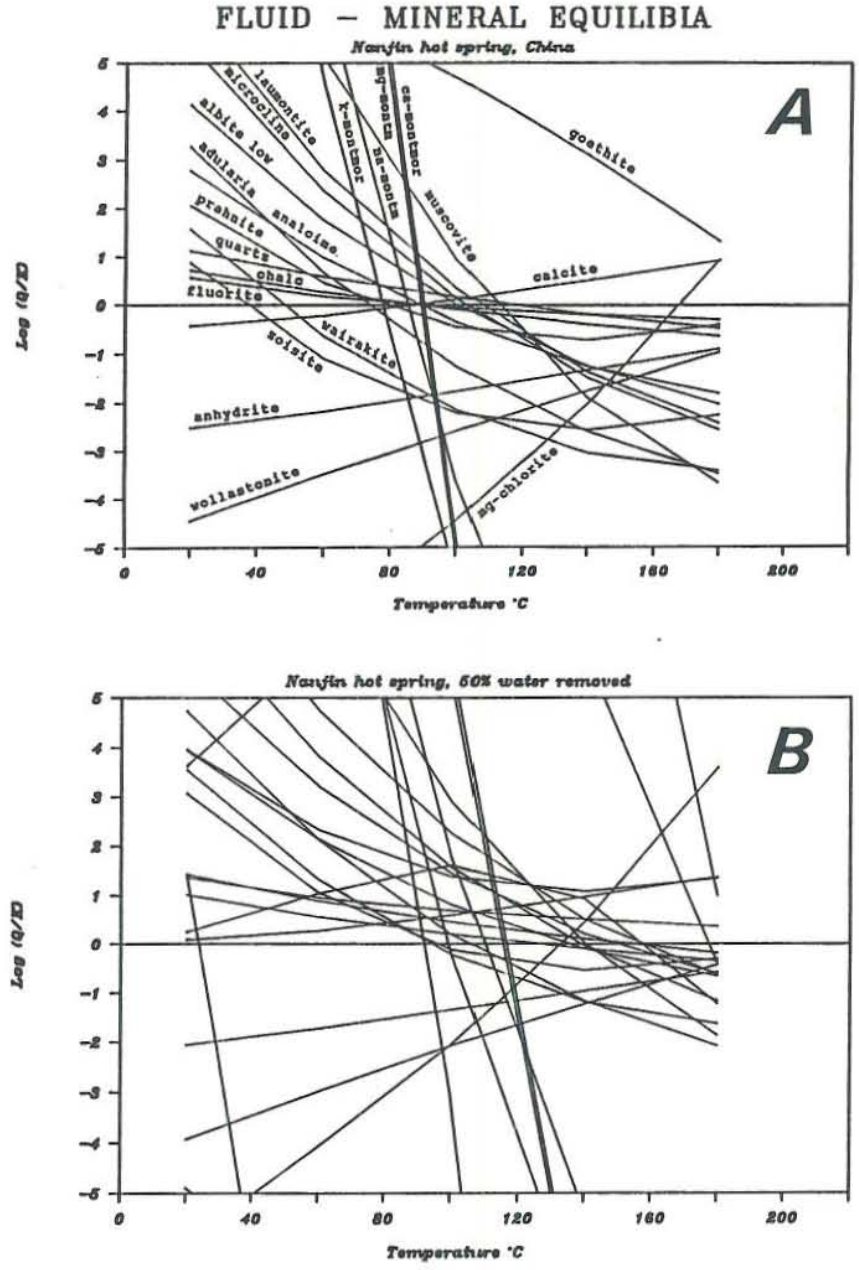

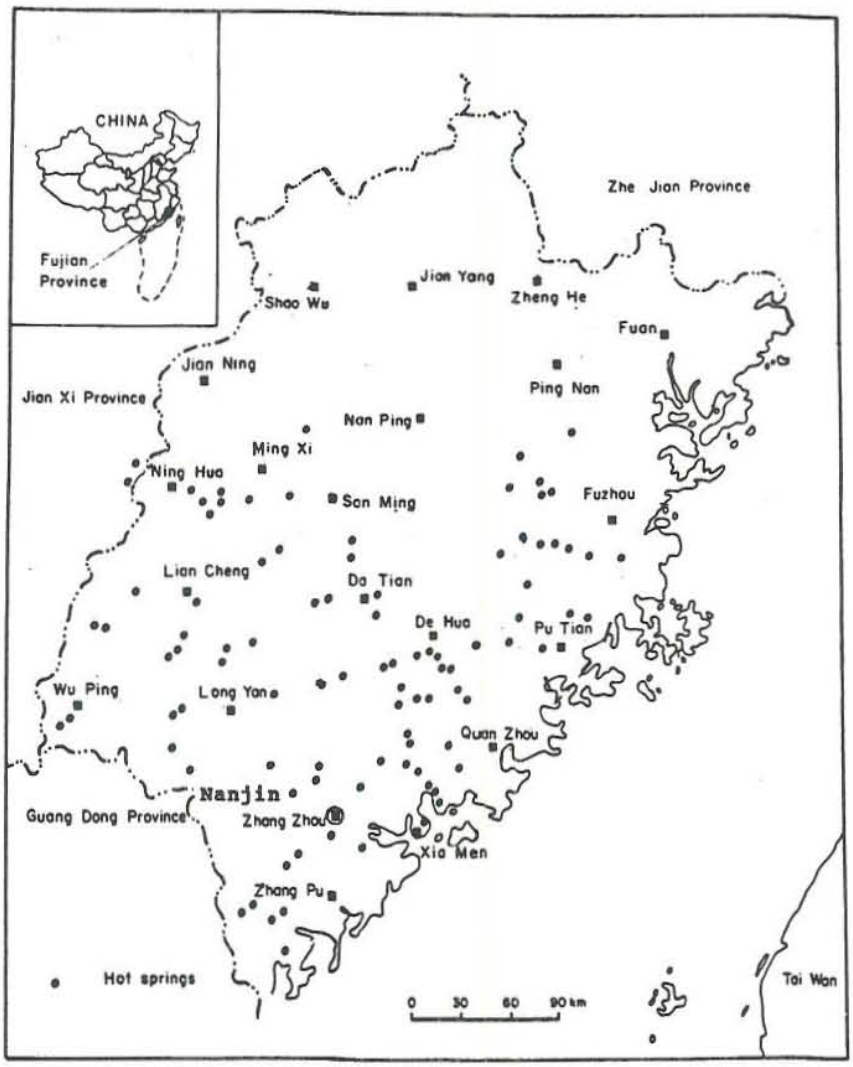

Figure 5.10 A map of Fujian Province, Southeast China showing the location of the Zhangzhou geothermal field and the surrounding areas where the Chinese samples were taken.

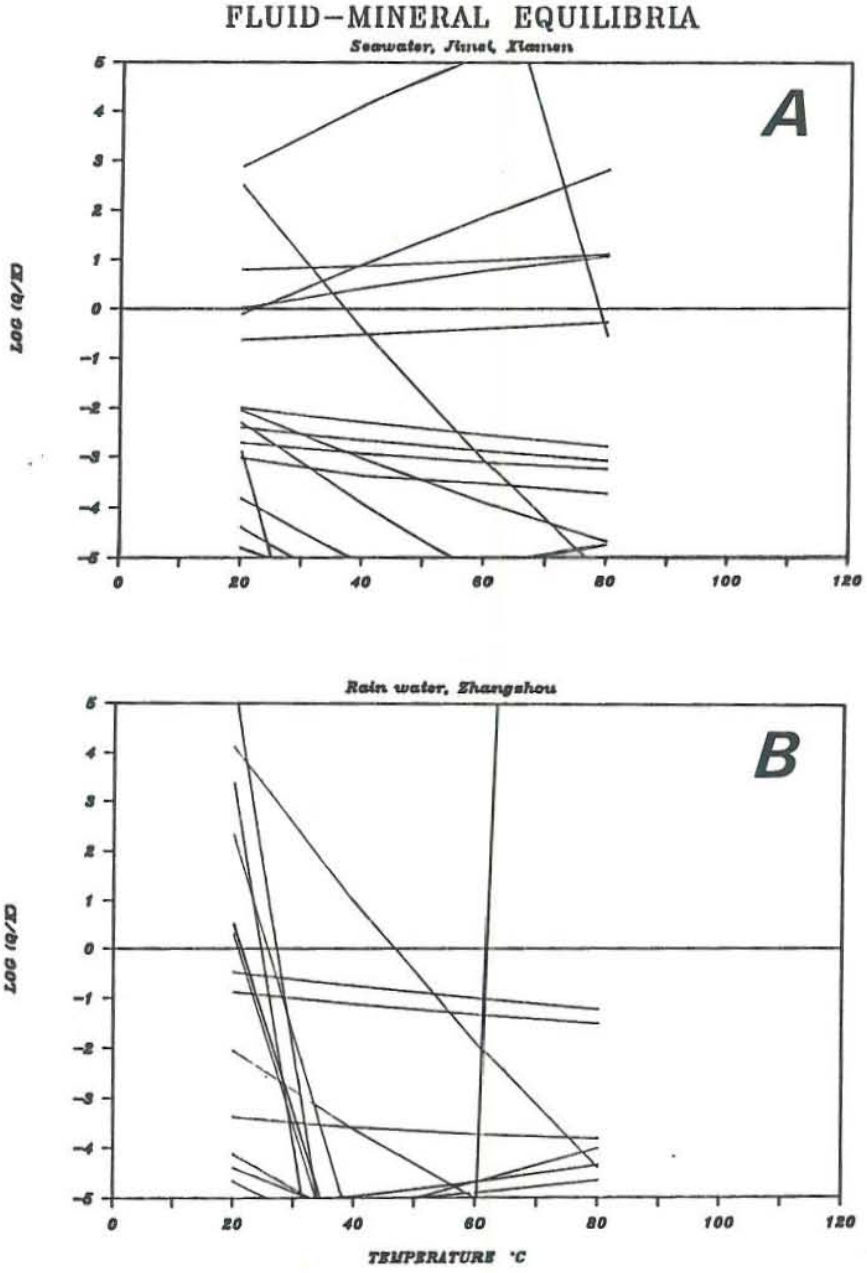

Figure 5.11 The log(Q/K) diagrams for seawater and rainwater from the Zhangzhou geothermal area and surroundings, Southeast China.

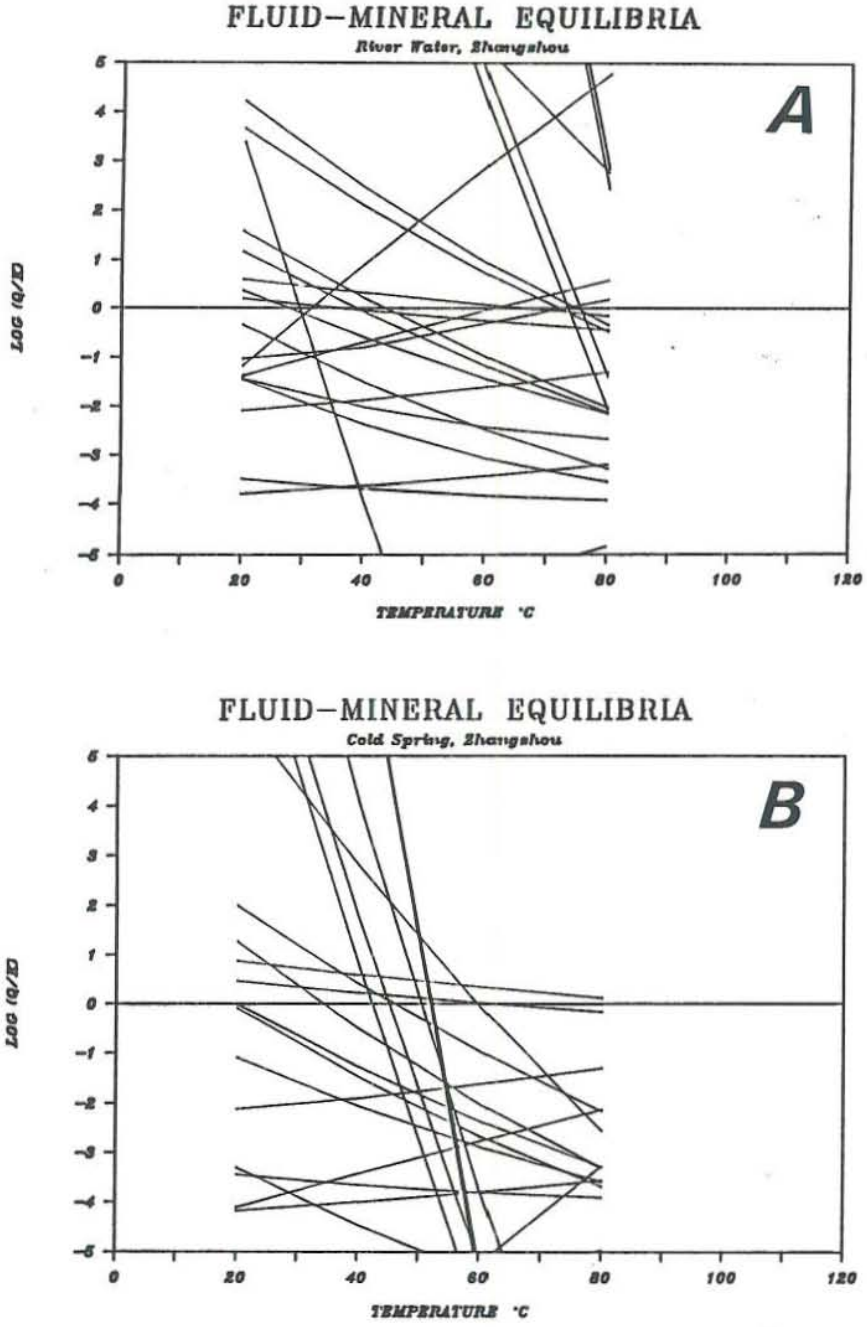

Figure 5.12 The log(Q/K) diagrams for riverwater and cold spring water from the Zhangzhou geothermal area and surroundings.

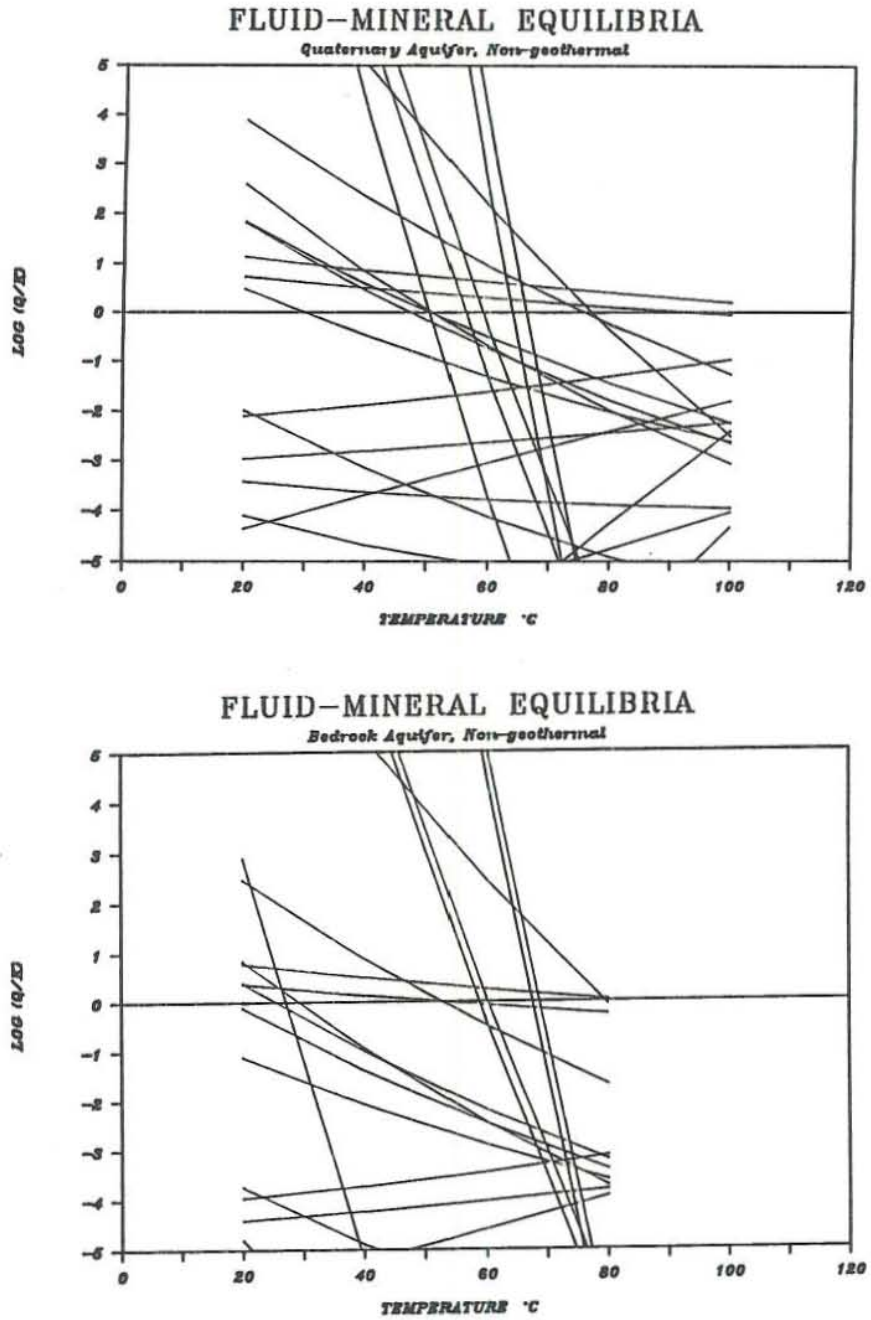

Figure 5.13 The log(Q/K) diagrams for groundwater of ambient temperature.

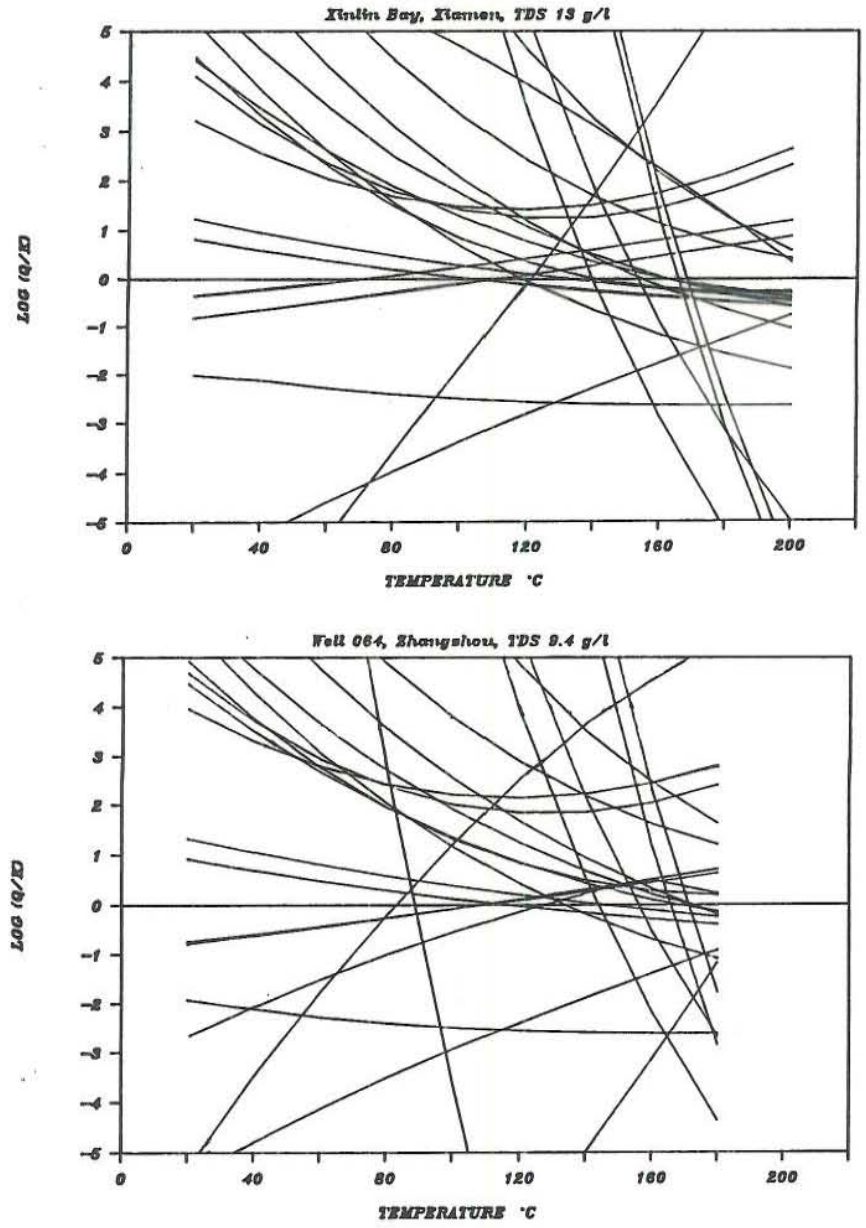

Figure 5.14 The log(Q/K) diagrams for some coastal geothermal water samples from the Zhangzhou area, which are chemically dominated by seawater.

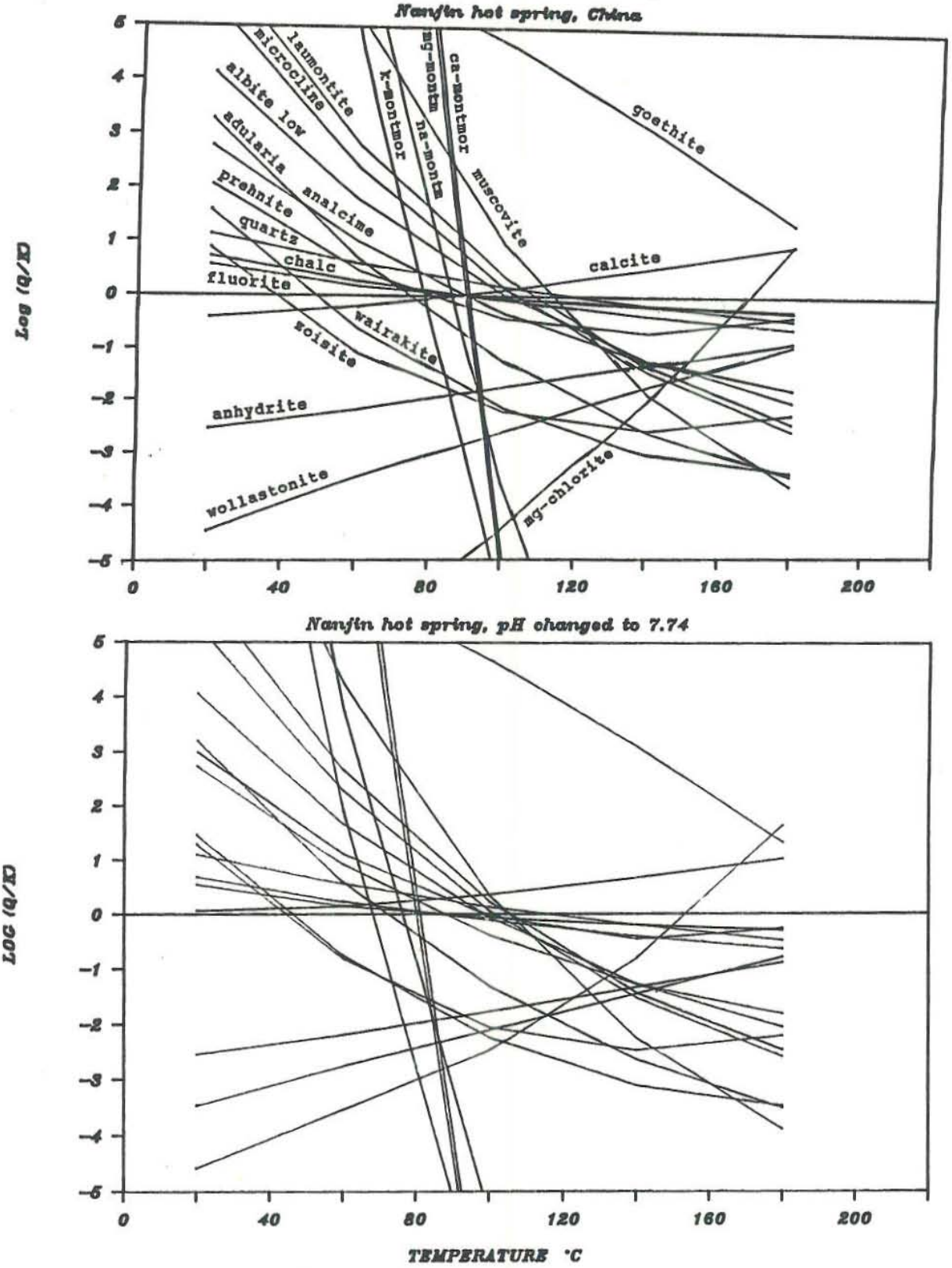

Figure 5.15 Log(Q/K) diagrams showing the effect of pH change by 0.5 units.

Figure 5.16. Statistical results of the evaluation of pH effect.

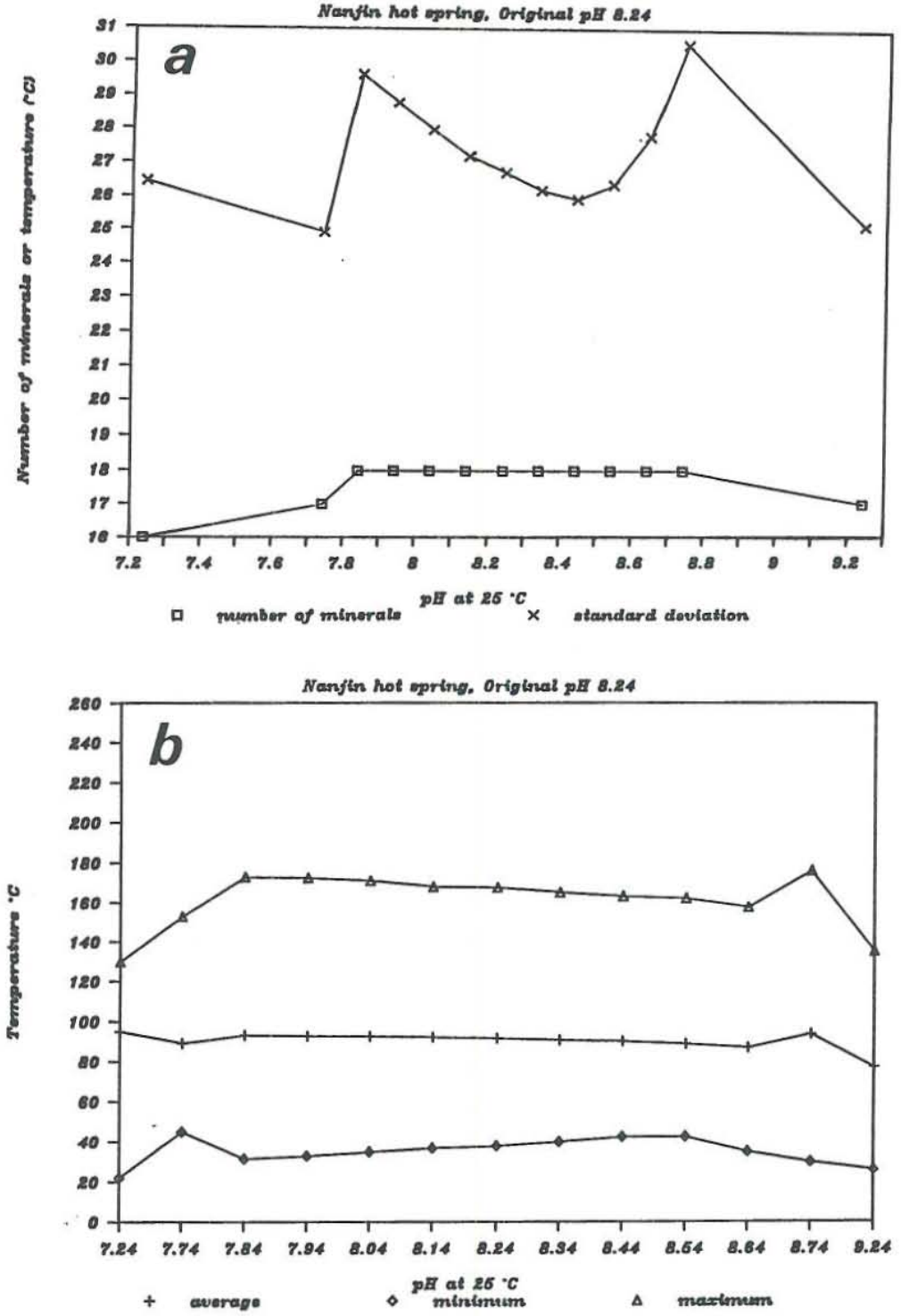

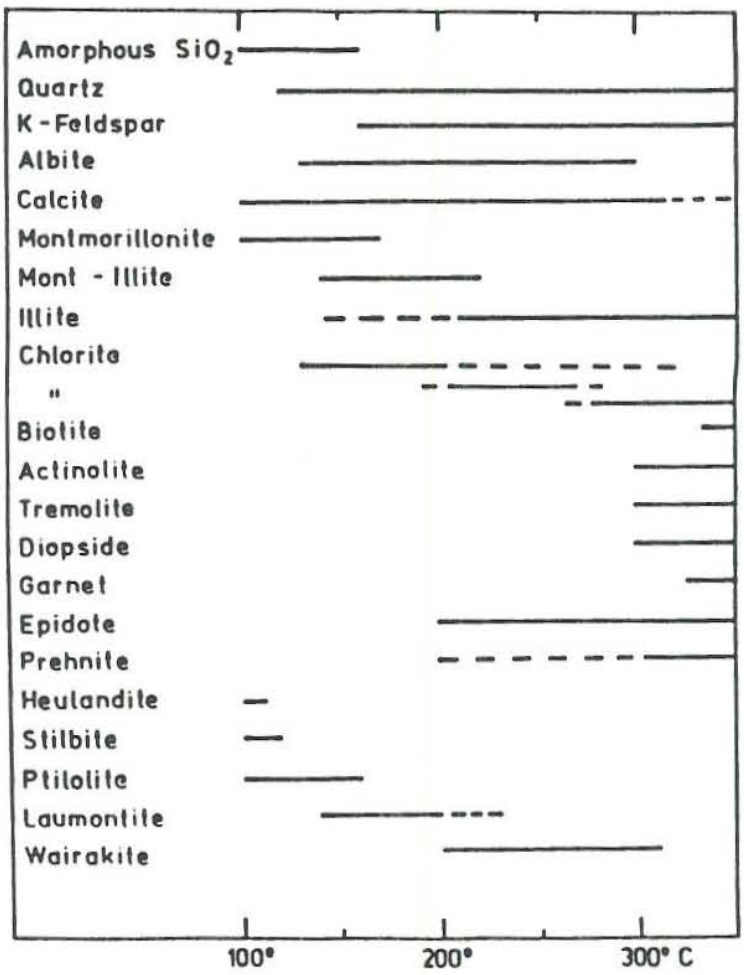

Figure 6.1 Distribution of some hydrothermal minerals in active geothermal systems (from Henley and Ellis, 1983).

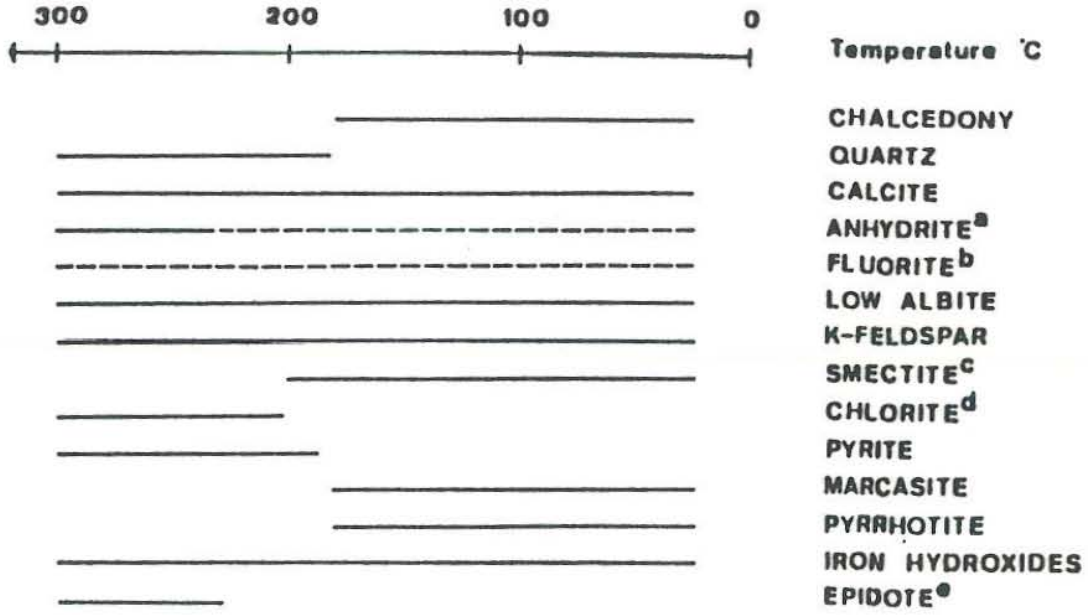

Figure 6.2 Distribution of minerals in geothermal systems in Iceland with which the water equilibrates(from Arnorsson et al., 1983).

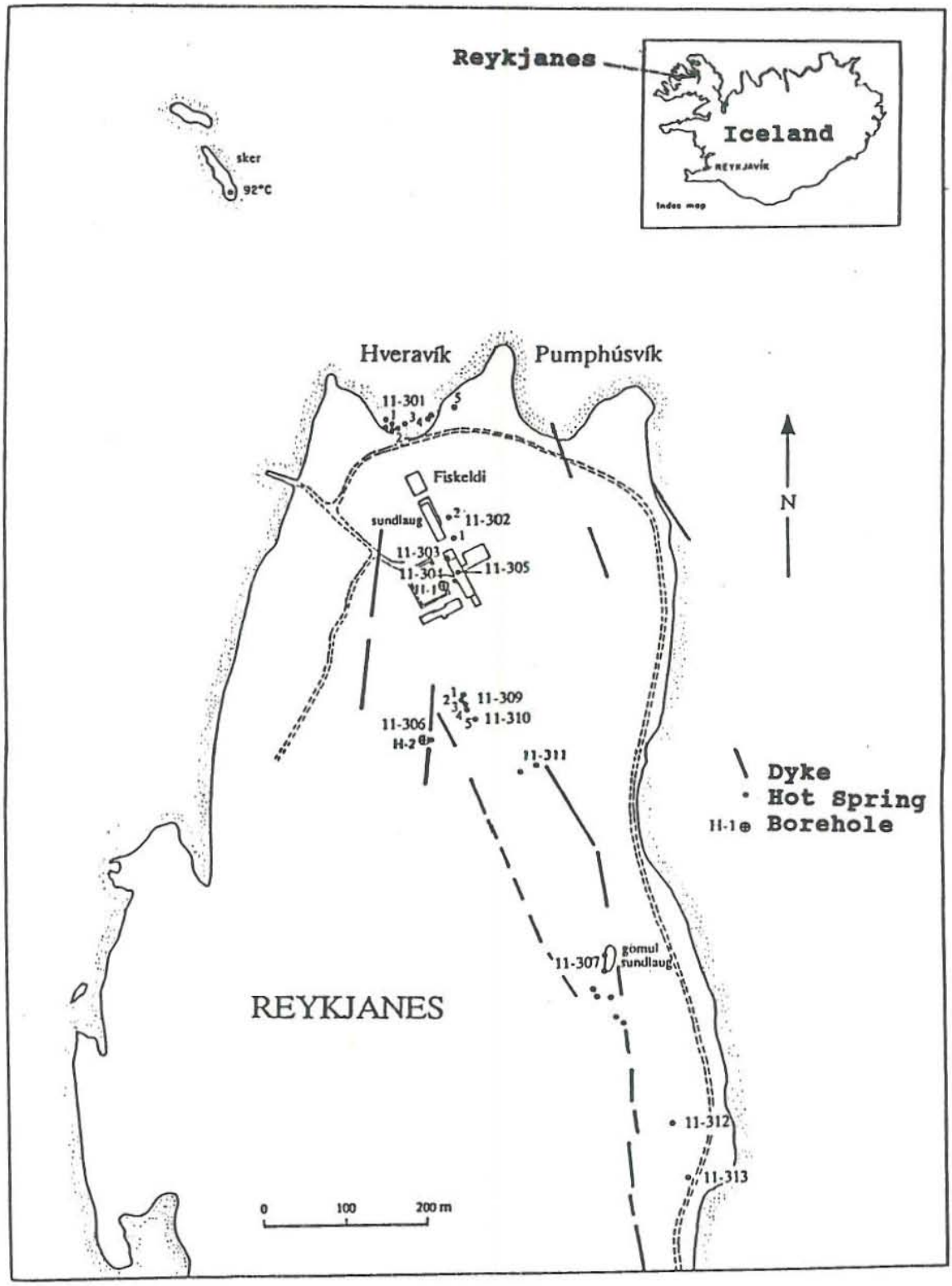

Figure 6.3 Location map of the Reykjanes area.

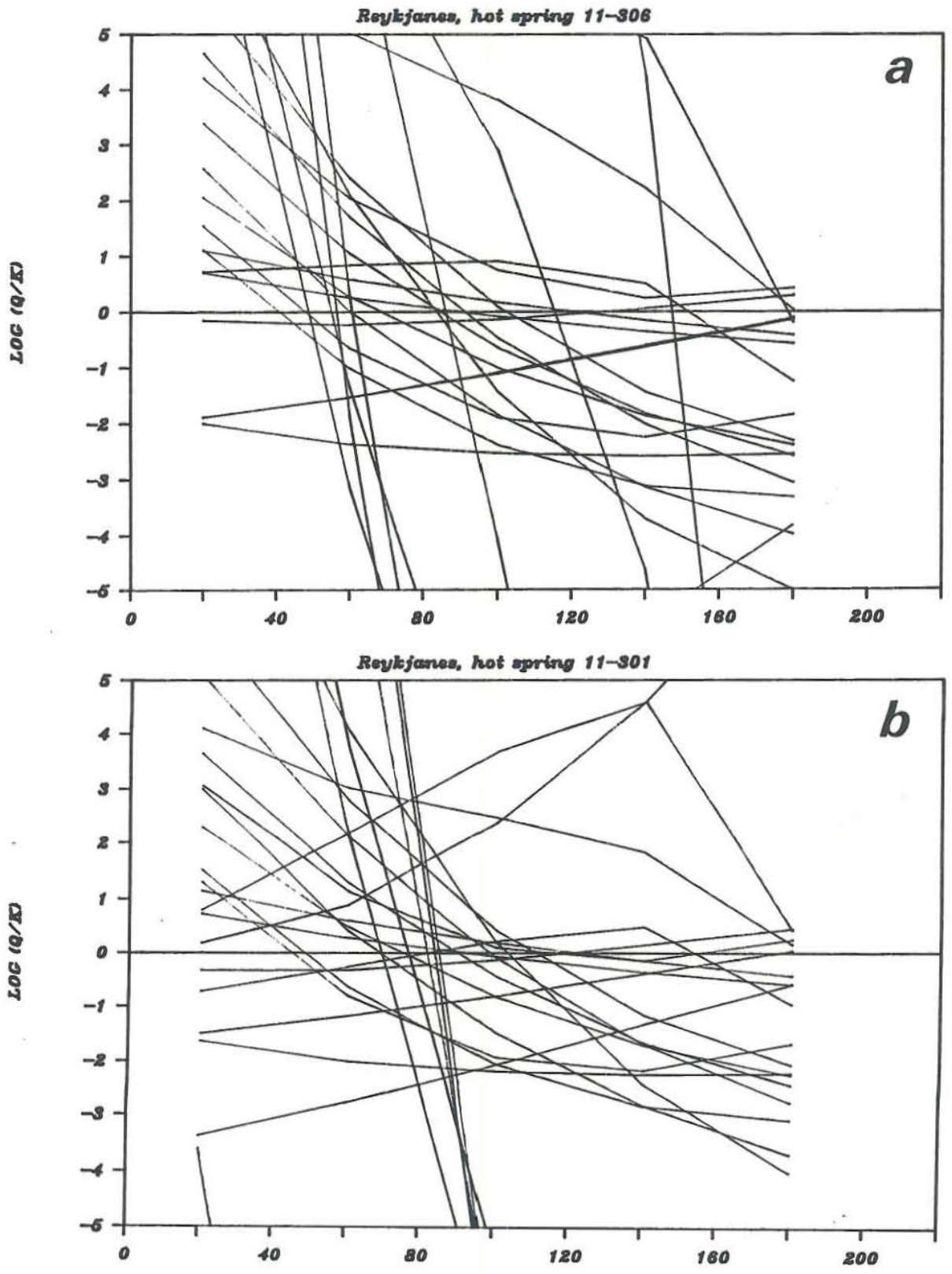

Figure 6.4 Log(Q/K) diagrams for samples from different parts of the system.

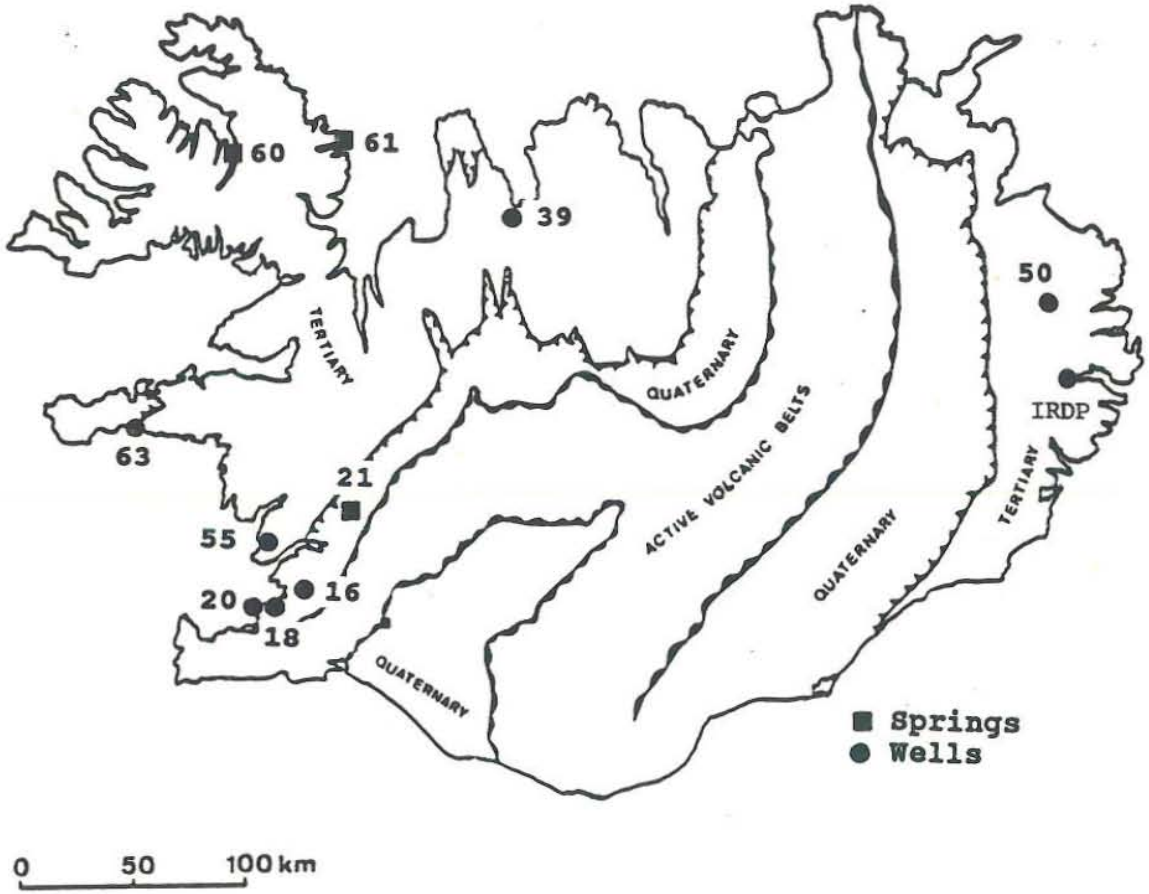

Figure 7.1 A map of Iceland showing the location of the samples selected for the calculations.

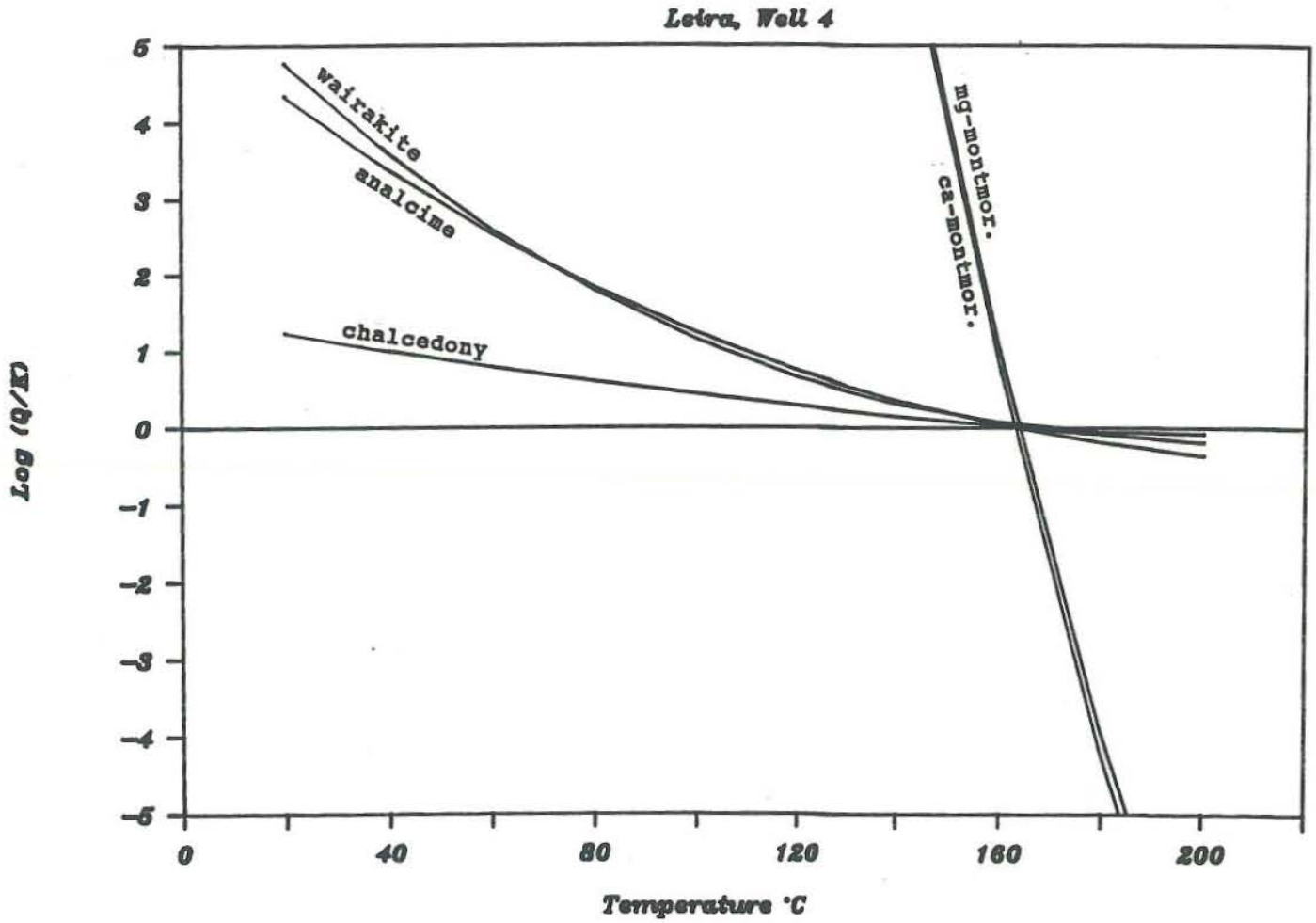

Figure 7.2 The log(Q/K) diagram for the Leira area.

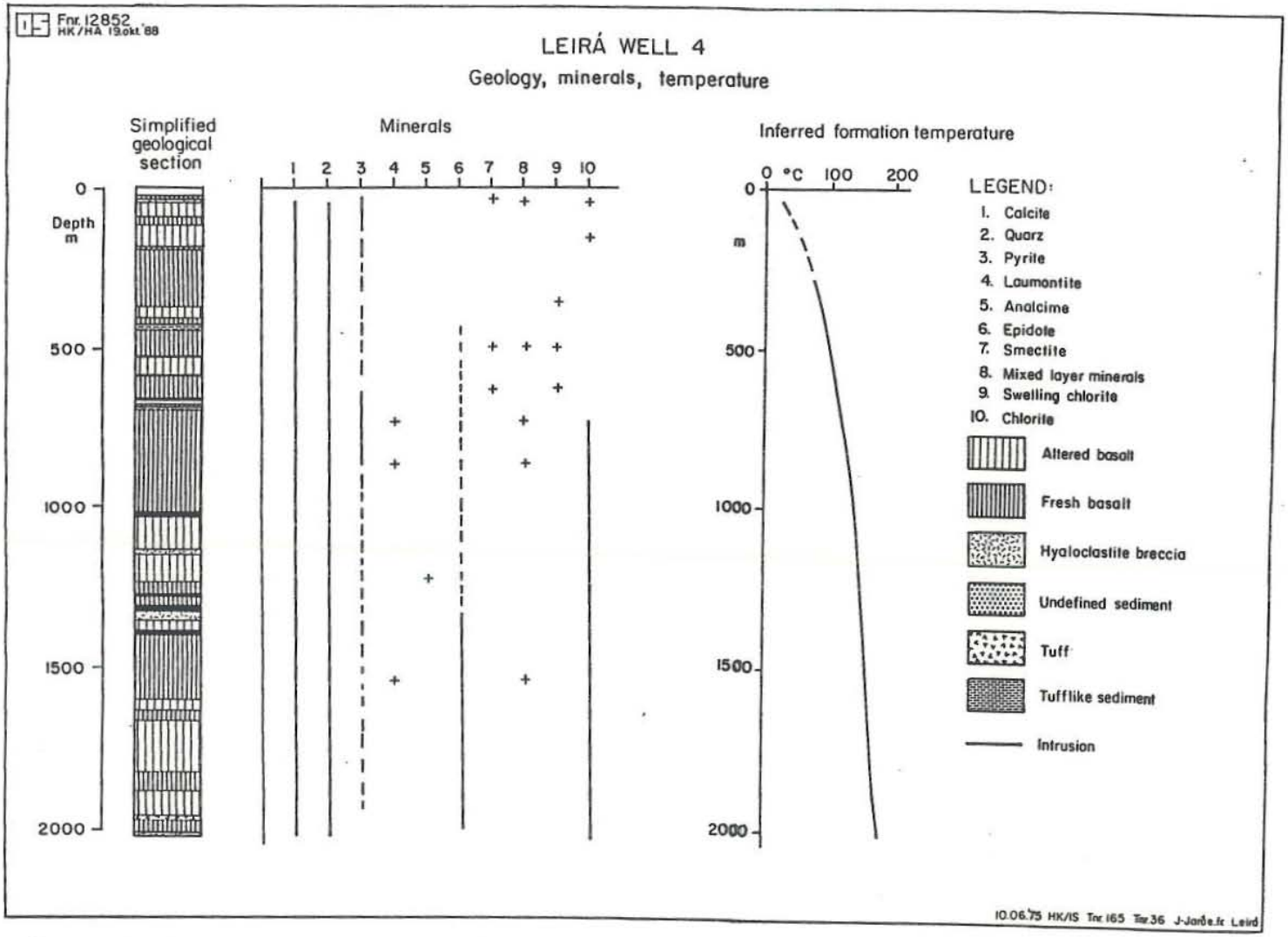

Figure 7.3 Geology, minerals and temperature in well 4, Leira area (from Tomasson and Kristmannsdottir, 1974).

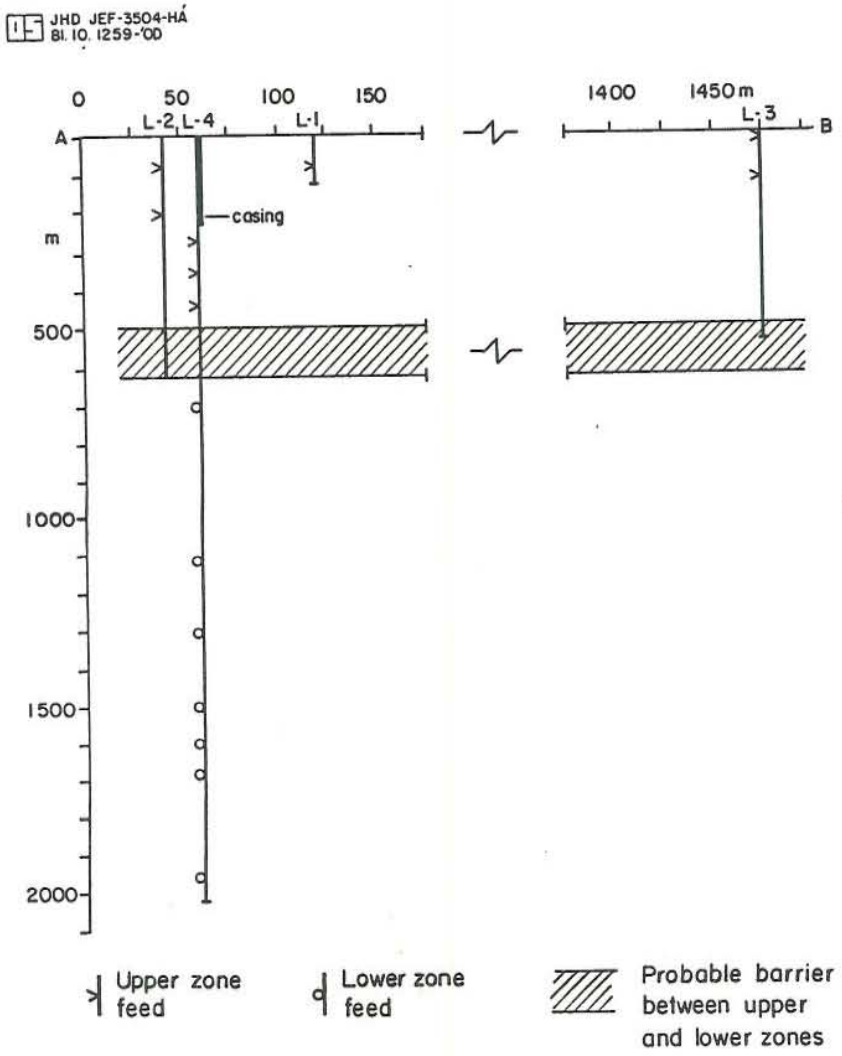

Figure 7.4 Depth and most important feeds of the Leira boreholes (from Armannsson, 1981).

Figure 7.5 The log(Q/K) diagram for the Nanjin hot spring area.

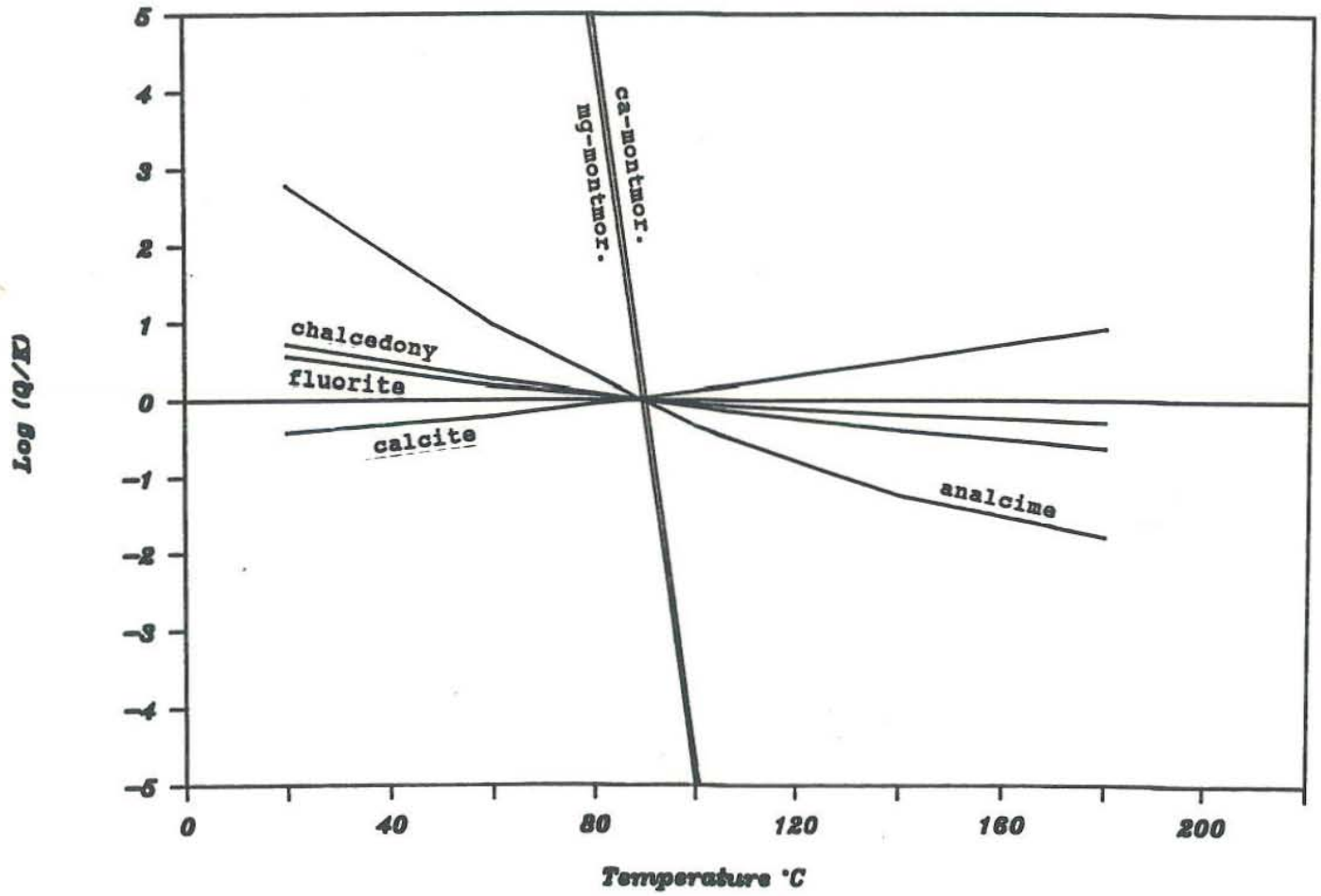

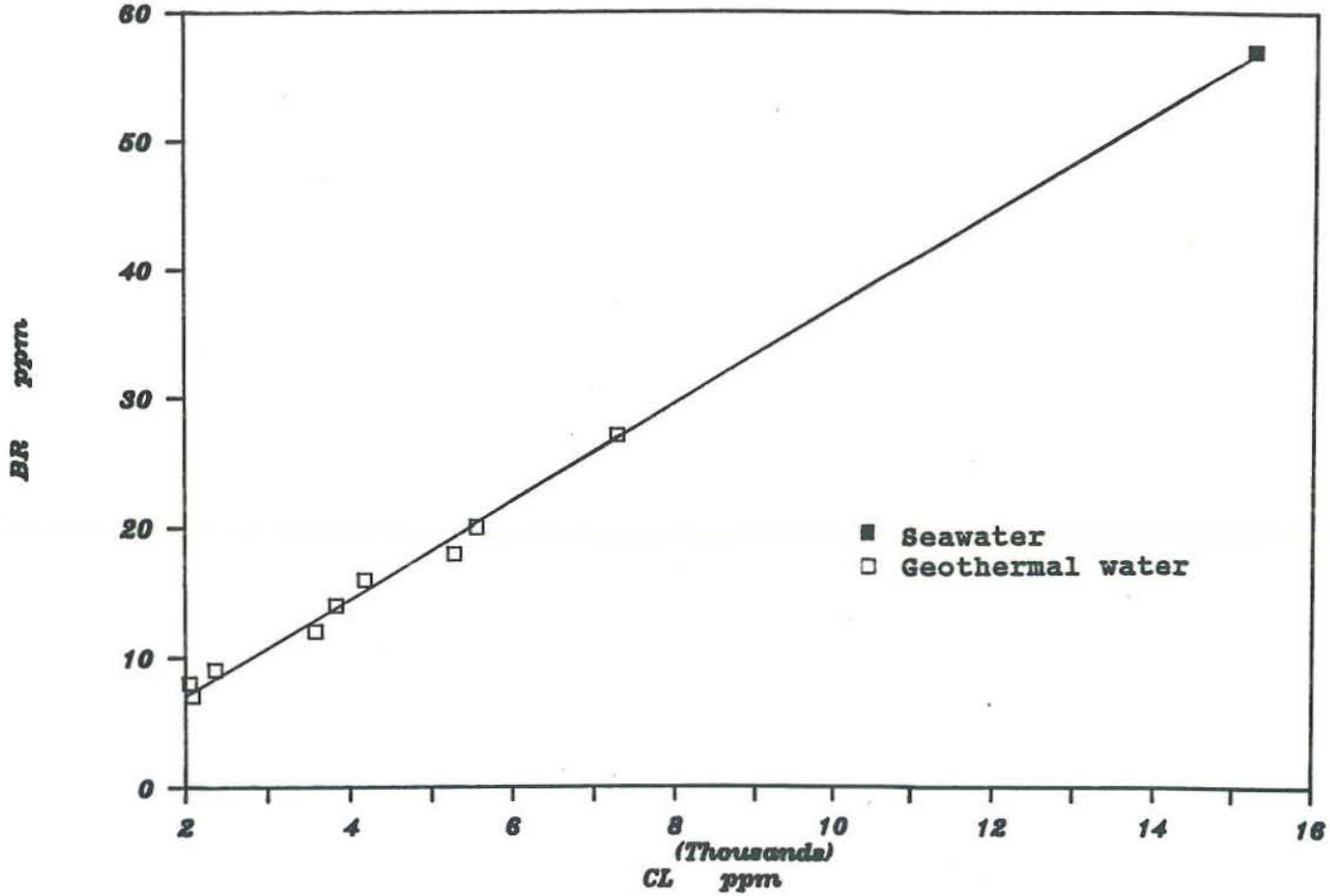

Figure 7.6 Cl - Br relation showing the mixing of meteoric water and seawater in the Zhangzhou geothermal area, Southeast China.

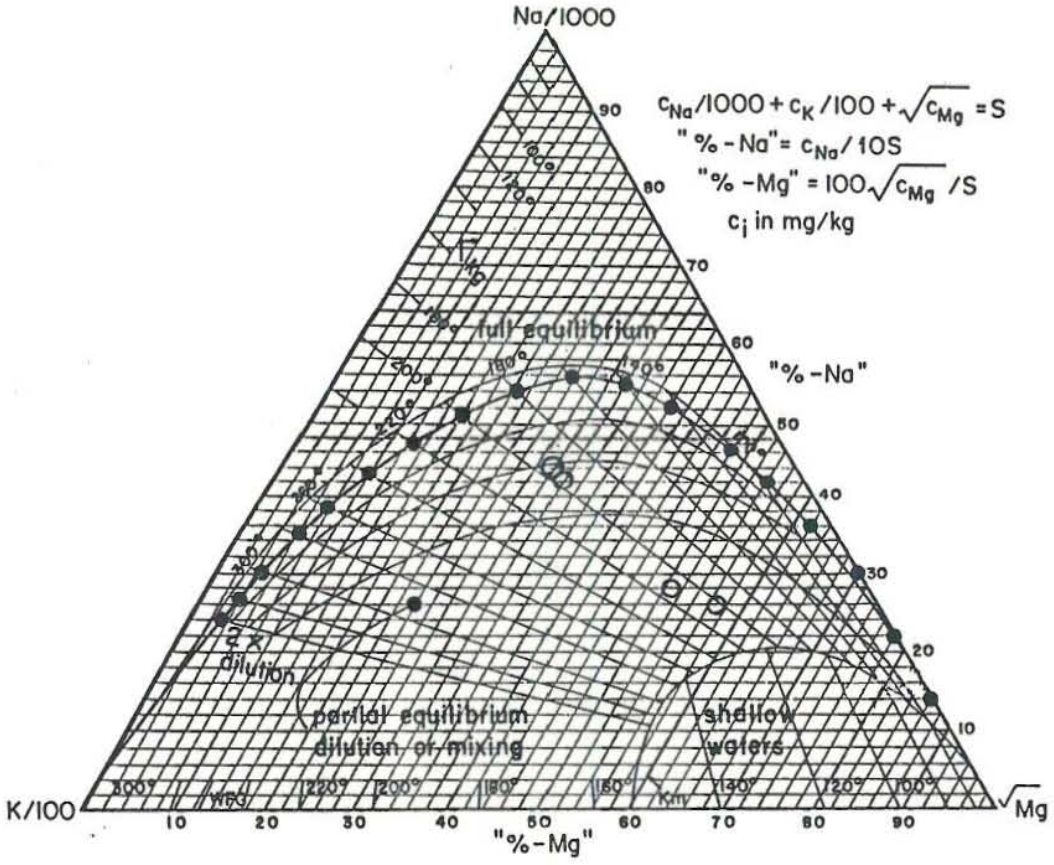

o **Geothermal water from the Zhangzhou geothermal field**

Figure 7.7 Giggenbach diagram for samples from the Zhangzhou geothermal area.